were performed. As shown in Fig. 3A, luciferase activity driven by p53-RE1 or p53-RE2 was significantly enhanced by co-expression with p53, whereas p53 had marginal effects on p53-RE3 and p53-RE4. To determine whether p53 could be recruited onto p53-RE1 and/or p53-RE2, we performed chromatin immunoprecipitation (ChIP) assays. H1299 cells were transfected with the empty plasmid or with the expression plasmid for p53. Forty-eight hours after transfection, cross-linked chromatin was immunoprecipitated with normal mouse serum (NMS) or with monoclonal antibody against p53 and subjected to PCR-based amplification. As shown in Fig. 3B, genomic fragment containing p53-RE1 or p53-RE2 was precipitated with anti-p53 antibody, suggesting that p53 is recruited onto p53-RE1 and p53-RE2 in cells. On the other hand, genomic fragment including p53-RE3 was not precipitated with anti-p53 antibody. Similarly, p53 was not recruited onto p53-RE4 (data not shown).

UNC5H4-mediated apoptosis is dependent on p53 status

We next examined whether UNC5H4 could induce apoptosis. *p53*-proficient U2OS and *p53*-deficient H1299 cells were transfected with the empty plasmid or with the expression plasmid for UNC5H4. Forty-eight hours after transfection, cells were maintained in fresh medium containing G418. After two weeks of selection, drug-resistant colonies were stained with Giemsa's solution. As shown in Fig. 4A, a significant decrease in number of drug-resistant colonies was observed in U2OS cells transfected with UNC5H4 expression plasmid relative to control cells, whereas UNC5H4 failed to show a significant effect on H1299 cells. Furthermore, UNC5H4-dependent induction of proteolytic cleavage of PARP was detected in U2OS cells, suggesting that UNC5H4-mediated decrease in number of drug-resistant colonies is attributed to the induction of apoptosis (Fig. 4B). Thus, it is likely that UNC5H4-mediated apoptosis is dependent on *p53* status.

To ask the functional significance of endogenous UNC5H4, we designed four siRNAs against UNC5H4 (#1, #2, #3 and #4). Among cell lines that we examined, osteosarcoma SAOS-2 cells express *UNC5H4* at the highest level (data not shown) and we used SAOS-2 cells to check the effectiveness of each of these siRNAs. Transfection of each of these siRNAs into SAOS-2 cells revealed that #1 and #3 siRNAs significantly down-regulate *UNC5H4* (Fig. 4C). Thus, we used #3 siRNA for further experiments. To address whether UNC5H4 could contribute to ADR-mediated apoptosis, U2OS cells were transfected with control siRNA or with #3 siRNA and exposed ADR. Forty-eight hours after ADR treatment, cells were analyzed for their cell cycle distributions by FACS. As shown in Fig. 4D, siRNA-mediated knockdown of UNC5H4 resulted in a decrease in number of cells with sub-G0/G1 DNA content relative to control cells, indicating that UNC5H4 plays an important role in the regulation of ADR-mediated apoptosis. Similar results were also obtained in U2OS cells transfected with #1 siRNA (data not shown).

Discussion

In the present study, we employed luciferase reporter assay and ChIP analysis to show that *UNC5H4* is a direct transcriptional target of p53 and its gene product has an apoptosis-inducing activity. Consistent with these results, ADR-mediated accumulation of p53 significantly correlates with transcriptional up-regulation of *UNC5H4* in U2OS cells. In contrast, ADR had undetectable effect on *UNC5H4* in p53-deficient H1299 cells. We have also found out several putative p53-binding sites in the 5′-upstream region of *UNC5H4*. Luciferase reporter assay demonstrated that these elements do not respond to exogenously expressed p53 (data not shown). Thus, we conclude that intronic p53-RE1 and p53-RE2 are genuine p53-responsive elements.

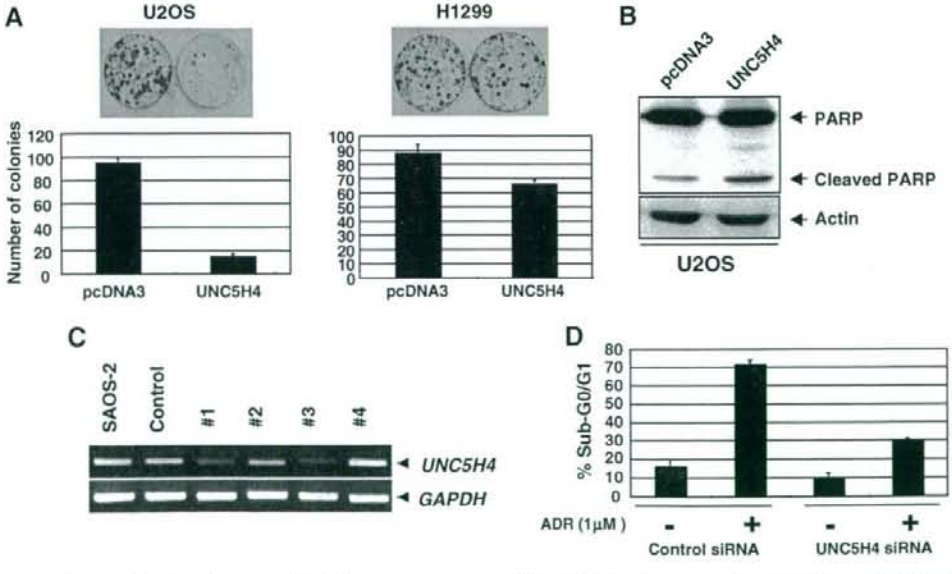

Fig. 4. UNC5H4-mediated apoptosis is dependent on p53. (A) Colony formation assay. U2OS and H1299 cells were transfected with the expression plasmid for UNC5H4. Forty-eight hours after transfection, cells were exposed to 400 μg/ml of G418 for two weeks. Drug-resistant colonies were then stained with Giemsa's solution. (B) Proteolytic cleavage of PARP. U2OS cells were transfected with the empty plasmid or with UNC5H4 expression plasmid. Forty-eight hours after transfection, cell lysates were prepared and processed for immunoblotting with anti-PARP antibody. (C) siRNA-mediated knockdown of UNC5H4. SAOS-2 cells were transfected with indicated siRNAs. Forty-eight hours after transfection, total RNA was prepared and subjected to RT-PCR. (D) siRNA-mediated knockdown of UNC5H4 renders U2OS cells resistant to ADR. U2OS cells were transfected with control siRNA or with siRNA against UNC5H4. Twenty-four hours after transfection, cells were treated with 1 μM of ADR. Forty-eight hours after ADR treatment, cells were stained with propidium iodide (PI) and their cell cycle distributions were analyzed by FACS.

Similar to the other UNC5H family members, UNC5H4 contains a canonical caspase cleavage site (413-DVID-416) [11] in its cytoplasmic region and enforced expression of UNC5H4 caused an apoptosis. Although it has been largely unknown how membrane UNC5H family proteins could transmit an apoptotic signal from cell surface to cytoplasm and/or nucleus, it is worth noting that UNC5H1–3 are cleaved by caspase-3 and treatment of cells with potent caspase inhibitor completely blocks UNC5H-mediated apoptosis [2], indicating that activated caspase-mediated proteolytic cleavage of cytoplasmic region of UNC5H including death domain plays an important role in the induction of apoptosis. Tanikawa et al. detected the cleaved fragment derived from UNC5H2 in cells infected with adenovirus encoding p53 [13]. Our preliminary results indicated that the cleaved fragment derived from UNC5H4 is detectable in both cytoplasm and nucleus of cells transfected with the expression plasmid for UNC5H4 (data not shown). Considering that UNC5H4-mediated induction of apoptosis is dependent on *p53* status, it is possible that functional interaction between p53 and cleaved fragment of UNC5H4 might take place in cell nucleus, and thereby amplifying p53-mediated apoptotic response. Further study should be required to address this issue.

Acknowledgments

We are grateful to Dr. H. Arakawa for valuable discussion. This work was supported in part by a Grant-in-Aid from the Ministry of Health, Labour and Welfare for the Third Term Comprehensive Control Research for Cancer, a Grant-in-Aid for Scientific Research on Priority Areas from the Ministry of Education, Culture, Sports, Science and Technology, Japan, a Grant-in-Aid for Scientific Research from Japan Society for the Promotion of Science, Uehara Memorial Foundation and Hisamitsu Pharmaceutical Co.

References

[1] P. Mehlen, S. Rabizadeh, S.J. Snipas, N. Assa-Munt, G.S. Salvesen, D.E. Bredesen, The DCC gene product induces apoptosis by a mechanism requiring receptor proteolysis, Nature 395 (1998) 801–804.
[2] F. Llambi, F. Causeret, E. Bloch-Gallego, P. Mehlen, Netrin-1 acts as a survival factor via its receptors UNC5H and DCC, EMBO J. 20 (2001) 2715–2722.
[3] P. Mehlen, D.E. Bredesen, The dependence receptor hypothesis, Apoptosis 9 (2004) 37–49.
[4] E.R. Fearon, K.R. Cho, J.M. Nigro, S.E. Kern, J.W. Simons, J.M. Ruppert, J.D. Oliner, K.W. Kinzler, B. Vogelstein, Identification of a chromosome 18q gene that is altered in colorectal cancers, Science 247 (1990) 49–56.
[5] E.R. Fearon, DCC: is there a connection between tumorigenesis and cell guidance molecules?, Biochim Biophys. Acta 1288 (1996) M17–M23.
[6] M. Tessier-Lavigne, C.S. Goodman, The molecular biology of axon guidance, Science 274 (1996) 1123–1133.
[7] E.D. Leonardo, I. Hinck, M. Masu, K. Keino-Masu, S.L. Ackerman, M. Tessier-Lavigne, Vertebrate homologues of *C. elegans* UNC-5 are candidate netrin receptors, Nature 386 (1997) 833–838.
[8] K. Hong, L. Hinck, M. Nishiyama, M.M. Poo, M. Tessier-Lavigne, E. Stein, A ligand-gated association between cytoplasmic domains of UNC5 and DCC family receptors converts netrin-induced growth cone attraction to repulsion, Cell 97 (1999) 927–941.
[9] N. Yokota, T.G. Mainprize, M.D. Taylor, T. Kohata, M. Loreto, S. Ueda, W. Dura, W. Grajkowska, J.S. Kuo, J.T. Rutka, Identification of differentially expressed and developmentally regulated genes in medulloblastoma using suppression subtraction hybridization, Oncogene 23 (2004) 3444–3453.
[10] K. Thiebault, L. Mazelin, L. Pays, F. Llambi, M.O. Joly, J.Y. Scoazec, J.C. Saurin, G. Romeo, P. Mehlen, The netrin-1 receptors UNC5H are putative tumor suppressors controlling cell death commitment, Proc. Natl. Acad. Sci. USA 100 (2003) 4173–4178.
[11] N.A. Thornberry, T.A. Rano, E.P. Peterson, D.M. Rasper, T. Timkey, M. Garcia-Calvo, V.M. Houtzager, P.A. Nordstrom, S. Roy, J.P. Vaillancourt, K.T. Chapmann, A combinatorial approach defines specificities of members of the caspase family and granzyme B. Functional relationships established for key mediators of apoptosis, J. Biol. Chem. 272 (1997) 17907–17911.
[12] M.E. Williams, P. Strickland, K. Watanabe, I. Hinck, UNC5H1 induces apoptosis via its juxtamembrane region through an interaction with NRAGE, J. Biol. Chem. 278 (2003) 17483–17490.
[13] C. Tanikawa, K. Matsuda, S. Fukuda, Y. Nakamura, H. Arakawa, p53RDL1 regulates p53-dependent apoptosis, Nat. Cell Biol. 5 (2003) 216–223.
[14] F. Llambi, F. Calheiros-Lourenco, D. Gozuacik, C. Guix, L. Pays, G. Del Rio, Kimchi, P. Mehlen, The dependence receptor UNC5H2 mediates apoptosis through DAP-kinase, EMBO J. 24 (2005) 1192–1201.
[15] T. Reveh, G. Droguertt, M.S. Horwitz, R.A. DePinho, A. Kimchi, DAP kinase activates a p19ARF/p53-mediated apoptotic checkpoint to suppress oncogenic transformation, Nat. Cell Biol. 3 (2001) 1–7.
[16] T. Ichikawa, Y. Suenaga, T. Koda, T. Ozaki, A. Nakagawara, TAp63-dependent induction of growth differentiation factor 15 (GDF15) plays a critical role in the regulation of keratinocyte differentiation, Oncogene 27 (2008) 409–420.
[17] K.H. Vousden, X. Lu, Live or let die: the cell's response to p53, Nat. Rev. Cancer 2 (2002) 594–604.
[18] T. Miyashita, J.C. Reed, Tumor suppressor p53 is a direct transcriptional activator of the human *bax* gene, Cell 80 (1995) 293–299.

THE JOURNAL OF BIOLOGICAL CHEMISTRY VOL. 283, NO. 13, pp. 8555–8563, March 28, 2008

Inhibitory Role of Plk1 in the Regulation of p73-dependent Apoptosis through Physical Interaction and Phosphorylation*[S]

Received for publication, December 31, 2007 Published, JBC Papers in Press, January 3, 2008, DOI 10.1074/jbc.M710608200

Nami Koida[‡§], Toshinori Ozaki[‡], Hideki Yamamoto[‡], Sayaka Ono[¶], Tadayuki Koda[¶], Kiyohiro Ando[‡], Rintaro Okoshi[‡], Takehiko Kamijo[‡], Ken Omura[§], and Akira Nakagawara[‡1]

From the [‡]Division of Biochemistry, Chiba Cancer Center Research Institute, Chiba 260-8717, the [§]Department of Oral and Maxillofacial Surgery, Tokyo Medical and Dental University, Tokyo 113-8549, and [¶]Center for Functional Genomics, Hisamitsu Pharmaceutical Company, Incorporated, Chiba 260-8717, Japan

In response to DNA damage, p73 plays a critical role in cell fate determination. In this study, we have found that Plk1 (polo-like kinase 1) associates with p73, phosphorylates p73 at Thr-27, and thereby inhibits its pro-apoptotic activity. During cisplatin-mediated apoptosis in COS7 cells in which the endogenous p53 is inactivated by SV40 large T antigen, p73 was induced to accumulate in association with a significant down-regulation of Plk1. Consistent with these observations, Plk1 reduced the stability of the endogenous p73. Immunoprecipitation and *in vitro* pulldown assay demonstrated that p73 binds to the kinase domain of Plk1 through its NH_2-terminal region. Luciferase reporter assay and reverse transcription-PCR analysis revealed that Plk1 is able to block the p73-mediated transcriptional activation. Of note, kinase-deficient Plk1 mutant (Plk1(K82M)) retained an ability to interact with p73; however, it failed to inactivate the p73-mediated transcriptional activation, suggesting that kinase activity of Plk1 is required for the inhibition of p73. Indeed, *in vitro* kinase assay indicated that p73 is phosphorylated at Thr-27 by Plk1. Furthermore, small interference RNA-mediated knockdown of the endogenous Plk1 in p53-deficient H1299 cells resulted in a significant increase in the number of cells with sub-G_1 DNA content accompanied by the up-regulation of p73 and pro-apoptotic $p53^{AIP1}$ as well as the proteolytic cleavage of poly(ADP-ribose) polymerase. Thus, our present results suggest that Plk1-mediated dysfunction of p73 is one of the novel molecular mechanisms to inhibit the p53-independent apoptosis, and the inhibition of Plk1 might provide an attractive therapeutic strategy for cancer treatment.

p73 is one of newly identified *p53* tumor suppressor gene family members (*p53*, *p73*, and *p63*) that encodes a nuclear transcription factor (1–3). Like the other *p53* family members, *p73* encodes multiple isoforms, including TA (transactivating), with distinct COOH-terminal extensions arising from alternative splicing events and ΔN (nontransactivating) variants generated by alternative promoter usage (2–4). ΔNp73 has an oncogenic potential (5) and displays a dominant-negative behavior toward TAp73 as well as wild-type p53 (6). TAp73 transactivates overlapping set of p53-target genes implicated in the induction of cell cycle arrest and/or apoptosis, and plays an important role in the regulation of DNA damage response, which is closely linked to its DNA binding activity. The initial studies demonstrated that TAp73 does not induce enough to accumulate in response to DNA damage arising from UV exposure or actinomycin D treatment (1); however, it has been shown that, in response to certain subset of DNA-damaging agents, TAp73 accumulates in the cell nucleus and exerts its pro-apoptotic function (7).

Accumulating evidence suggests that TAp73 is regulated by post-translational modifications such as phosphorylation and acetylation. For example, TAp73 is stabilized in response to DNA damage such as cisplatin (CDDP)[2] treatment or exposure to γ-irradiation through the phosphorylation at Tyr-99 mediated by c-Abl (8–10). Ren *et al.* (11) demonstrated that protein kinase Cδ catalytic fragment phosphorylates TAp73 at Ser-289 in response to CDDP and thereby enhances its stability and activity. Further studies revealed that CDDP-mediated apoptosis is associated with phosphorylation of TAp73 at Ser-47 catalyzed by Chk1 (12). According to their results, Chk1-mediated phosphorylation of TAp73 resulted in an increase in its transcriptional activity. On the other hand, Gaiddon *et al.* (13) described that cyclin-dependent kinase phosphorylates TAp73 at Thr-86 and thereby reduces its transcriptional activity, suggesting that phosphorylation of TAp73 might not always convert a latent form of TAp73 to an active one. Additionally, several lines of evidence suggest that acetylation of TAp73 mediated by p300/CBP results in its activation (14). Constanzo *et al.* (15) reported that p300 has an ability to acetylate TAp73 at Lys-321, Lys-327, and Lys-331 in response to DNA damage in a c-Abl-dependent manner, and acetylated forms of TAp73 exert its pro-apoptotic function.

* This work was supported in part by a grant-in-aid from the Ministry of Health, Labor, and Welfare for Third Term Comprehensive Control Research for Cancer, a grant-in-aid for scientific research on priority areas from the Ministry of Education, Culture, Sports, Science, and Technology, Japan, a grant-in-aid for scientific research from Japan Society for the Promotion of Science, and a grant from Uehara Memorial Foundation. The costs of publication of this article were defrayed in part by the payment of page charges. This article must therefore be hereby marked "*advertisement*" in accordance with 18 U.S.C. Section 1734 solely to indicate this fact.

[S] The on-line version of this article (available at http://www.jbc.org) contains supplemental Figs. S1–S5.

[1] To whom correspondence should be addressed. Tel.: 81-43-264-5431; Fax: 81-43-265-4459; E-mail: akiranak@chiba-cc.jp.

[2] The abbreviations used are: CDDP, cisplatin; DAPI, 4, 6-diamidino-2-phenylindole; FACS, fluorescence-activated cell sorter; *GAPDH*, glyderaldehyde-3-phosphate dehydrogenase; GST, glutathione *S*-transferase; IB, immunoblotting; IP, immunoprecipitation; NMS, normal mouse serum; PARP, poly(ADP-ribose) polymerase; PBS, phosphate-buffered saline; RT, reverse transcription; siRNA, small interference RNA; GFP, green fluorescent protein.

Plk1 (Polo-like kinase 1) is a positive cell cycle regulator (16–18). Plk1 has an NH_2-terminal Ser/Thr protein kinase domain and tandem repeats of so-called "Polo-box motif" in its COOH-terminal region that might act as a phosphopeptide-binding domain (19). It has been shown that *Plk1* is overexpressed in a variety of human tumors as compared with their corresponding normal tissues (20, 21). Indeed, enforced expression of Plk1 in mouse fibroblasts causes oncogenic focus formation and promotes tumor growth in nude mice (22), suggesting that Plk1 has an oncogenic potential. In support with this notion, knockdown of the endogenous Plk1 induces G_2/M cell cycle arrest and/or apoptosis in various cell lines (23–25). Furthermore, it has been shown that Plk1 is inhibited in response to DNA damage in a mutated in ataxia telangiectasia (ATM) and ATM related kinase-dependent manner (26, 27), indicating that Plk1 is one of targets of DNA damage response. In this regard, we have found that Plk1 inhibits pro-apoptotic function of p53 through the physical interaction with it (20). Recently, Liu *et al.* (28) reported that Plk1 depletion promotes apoptosis of cancerous cells in a p53-independent manner. In this study, we have found that Plk1 has an ability to bind to and phosphorylate TAp73 at Thr-27, thereby inhibiting its transcriptional as well as pro-apoptotic activity.

EXPERIMENTAL PROCEDURES

Cell Lines and Transfection—African green monkey kidney COS7, human osteosarcoma SAOS-2, U2OS, and human cervical carcinoma HeLa cells were maintained in Dulbecco's modified Eagle's medium supplemented with 10% heat-inactivated fetal bovine serum (Invitrogen), 50 μg/ml penicillin, and 50 μg/ml streptomycin (Invitrogen). Human lung carcinoma H1299 cells were grown in RPMI 1640 medium supplemented with 10% heat-inactivated fetal bovine serum plus antibiotics mixture. These cells were cultured in a 5% CO_2 environment at 37 °C. Where indicated, cells were exposed to CDDP (Sigma). For transient transfection, COS7 and H1299 cells were transfected with the indicated combinations of the expression plasmids using Lipofectamine 2000 transfection reagent (Invitrogen) according to the manufacturer's instructions. pcDNA3 (Invitrogen) was used as a blank plasmid to balance the amount of DNA introduced in transient transfection.

RNA Extraction and RT-PCR—Total RNA was prepared from the indicated cells by using the RNeasy mini kit (Qiagen, Valencia, CA) according to the manufacturer's protocol and reverse-transcribed. The specific primers used were as follows: *p73α*, 5′-TCTGGAACCAGACAGCACCT-3′ and 5′-GTGCTGGACTGCTGGAAAGT-3′; $p21^{WAF1}$, 5′-ATGAAATTCACCCCCTTTCC-3′ and 5′-CCCTAGGCTGTGCTCACTTC-3′; *BAX*, 5′-TTTGCTTCAGGGTTTCATCC-3′ and 5′-CAGTTGAAGTTGCCGTCAGA-3′; *MDM2*, 5′-ACTTGAGCCGAGGAGTTCAA-3′ and 5′-TTGCTCTGTCACCTGGACTG-3′; *Plk1*, 5′-ATCACCTGCCTGACCATTCCACCAAGG-3′ and 5′-AATTGCGGAAATATTTAAGGAGGGTGATCT-3′; $p53^{AIP1}$, 5′-GATCTTCCTCTGAGGCGAGCT-3′ and 5′-TTACCCAGCCAGGTGTGTGT-3′; and *GAPDH*, 5′-ACCTGACCTGCCGTCTAGAA-3′ and 5′-TCCACCACCCTGTTGCTGTA-3′. The expression of *GAPDH* was measured as an internal control.

Immunoblotting—Whole cells lysates were prepared by incubating cells in lysis buffer containing 25 mM Tris-HCl, pH 8.0, 137 mM NaCl, 2.7 mM KCl, 1% Triton X-100 and a commercial protease inhibitor mixture (Sigma) for 30 min on ice and subjected to a brief sonication for 10 s at 4 °C followed by centrifugation at 15,000 rpm at 4 °C for 10 min to remove insoluble materials. The protein concentrations were measured using the Bradford protein assay according to the manufacturer's instructions (Bio-Rad). The equal amounts of protein (50 μg) were separated by 10% SDS-PAGE and electrophoretically transferred onto polyvinylidene difluoride membranes (Immobilon-P, Millipore, Bedford, MA). The transferred membranes were blocked with Tris-buffered saline containing 5% nonfat dry milk and 0.1% Tween 20 at 4 °C overnight. After blocking, the membranes were incubated with monoclonal anti-p73 (Ab-4; NeoMarkers, Fremont, CA), monoclonal anti-FLAG (M2; Sigma), monoclonal anti-Plk1 (PL2 and PL6; Zymed Laboratories Inc.), monoclonal anti-PARP (F-2; Santa Cruz Biotechnology, Santa Cruz, CA), polyclonal anti-p300 (H-272; Santa Cruz Biotechnology), or with polyclonal anti-actin (20–33; Sigma) antibody for 1 h at room temperature. After incubation with primary antibodies, the membranes were incubated with horseradish peroxidase-coupled goat anti-mouse or anti-rabbit IgG secondary antibody (Cell Signaling, Beverly, MA) for 1 h at room temperature. Immunoblots were visualized by ECL detection reagents according to the manufacturer's instructions (Amersham Biosciences).

Immunoprecipitation—HeLa cells were treated with CDDP at a final concentration of 20 μM. Twenty-four hours after CDDP treatment, whole cell lysates (1 mg of protein) were precleared with 30 μl of protein G-Sepharose beads and used for immunoprecipitation with the appropriate antibodies. After the addition of 30 μl of protein G-Sepharose beads, incubations were continued for additional 2 h at 4 °C. The beads were then collected by centrifugation and washed three times with the lysis buffer. The precipitated proteins were analyzed by 10% SDS-PAGE and immunoblotting with the appropriate antibodies as described.

GST Pulldown Assay—cDNA fragments encoding the indicated deletion mutants of p73α were generated by PCR-based strategy, and subcloned into GST fusion protein expression plasmid pGEX-4T-3 (Amersham Biosciences). GST and GST-p73α fusion proteins were expressed and purified by glutathione-Sepharose beads (Amersham Biosciences). FLAG-Plk1 was radiolabeled *in vitro* by using TnT QuickCoupled transcription/translation system (Promega, Madison, WI) in the presence of [^{35}S]methionine and incubated with GST or GST-p73α deletion mutants for 2 h at 4 °C. After the addition of 30 μl of glutathione-Sepharose beads into the reaction mixture, incubations were continued for 1 h at 4 °C. The beads were collected by centrifugation and washed three times with binding buffer containing 50 mM Tris-HCl, pH 7.5, 150 mM NaCl, 0.1% Nonidet P-40, and 1 mM EDTA. The ^{35}S-labeled bound proteins were eluted by 2× SDS sample buffer and separated by 10% SDS-PAGE. After electrophoresis, the gel was dried and exposed to an x-ray film with an intensifying screen.

Indirect Immunofluorescence Staining—HeLa cells were fixed in 3.7% formaldehyde for 30 min at room temperature,

permeabilized in 0.2% Triton X-100 for 5 min at room temperature, and then blocked with 3% bovine serum albumin in PBS for 1 h at room temperature. After blocking, cells were washed in PBS and incubated with polyclonal anti-p73 antibody (H-79; Santa Cruz Biotechnology) and monoclonal anti-Plk1 antibody for 1 h at room temperature, followed by the incubation with fluorescein isothiocyanate-conjugated anti-rabbit IgG and rhodamine-conjugated anti-mouse IgG (Invitrogen) for 1 h at room temperature. Cell nuclei were stained with DAPI.

Flow Cytometry—After transfection, both floating and attached cells were collected by low speed centrifugation, washed in PBS, and fixed in 70% ethanol at −20 °C overnight. The cells were then stained with propidium iodide (50 μg/ml) in the presence of 50 μg/ml RNase A for 30 min at room temperature. The DNA content indicated by propidium iodide staining was analyzed by FACSCalibur flow cytometer (BD Biosciences).

Luciferase Reporter Assay—p53-deficient H1299 cells were plated in 12-well plates at a density of 50,000 cells/well and transiently co-transfected with a constant amount of a luciferase reporter construct driven by p53/p73-responsive element derived from $p21^{WAF1}$, *Mdm2*, or *Bax* promoter, *Renilla* luciferase expression plasmid (pRL-TK), and the HA-p73α expression plasmid together with or without the increasing amounts of the expression plasmid for Plk1. Forty-eight hours after transfection, cells were lysed, and their luciferase activities were measured by dual luciferase reporter assay system (Promega). The firefly luminescence signal was normalized based on the *Renilla* luminescence signal. Each experiment was performed at least three times in triplicate.

Apoptotic Assay—H1299 cells were transfected with the indicated combinations of the expression plasmids. Forty-eight hours after transfection, cells were washed in PBS, fixed in 3.7% formaldehyde for 1 h at room temperature, and then permeabilized with 0.1% Triton X-100 for 5 min on ice. The cell nuclei were stained by DAPI. The number of GFP-positive cells with apoptotic nuclei was counted.

Construction of Mutant Forms of GST-p73α-(1–130)—To identify possible phosphorylation site(s) of p73α mediated by Plk1, the T27A mutation was introduced into the GST-p73α-(1–130) using PfuUltra™ high fidelity DNA polymerase (Stratagene, La Jolla, CA) according to the manufacturer's instructions. Details are available upon request. Nucleotide sequences of the PCR products were determined to verify the presence of the desired mutation and the absence of random mutations.

In Vitro Kinase Reaction—To identify the possible Thr residue(s) of p73α that could be phosphorylated by Plk1, we used CycLex Polo-like kinase 1 assay kit (CycLex, Nagano, Japan) (29). In brief, the purified Plk1 was added to the reaction mixture containing 50 μM ATP and polyclonal anti-phospho-Thr antibody and incubated for 30 min at room temperature. After the incubation, horseradish peroxidase-conjugated anti-rabbit IgG secondary antibody was mixed with the reaction mixture and incubated for 30 min at room temperature. Finally, GST or the indicated GST-p73α deletion mutants dissolved in substrate solution were added into the reaction mixture and incubated for 5 min at room temperature, followed by the measurement of absorbance in each well using a spectrophotometric plate reader at dual wavelength of 450/540 nm. As a positive control, we used protein X that was supplied by the manufacturer.

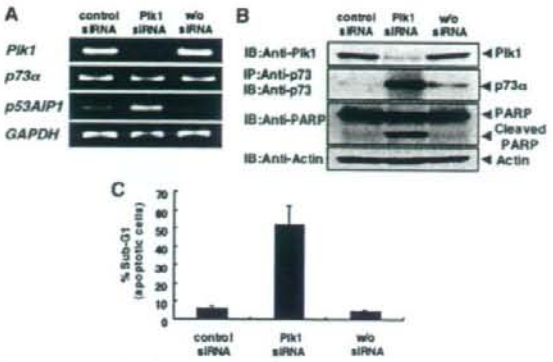

FIGURE 1. **siRNA-mediated knockdown of Plk1 induces apoptosis in p53-deficient H1299 cells.** *A*, siRNA-mediated knockdown of the endogenous *Plk1*. H1299 cells were transfected with control siRNA or with Plk1 siRNA (Plk1 siRNA). Forty-eight hours after transfection, total RNA was prepared and subjected to RT-PCR to examine the expression levels of *Plk1*, *p73α*, and $p53^{AIP1}$. *GAPDH* was used as an internal control. *B*, immunoblotting analysis. H1299 cells were transfected as in *A*. Forty-eight hours after transfection, whole cell lysates were prepared and processed for immunoblotting (*IB*) with the indicated antibodies. For the detection of the endogenous p73α, whole cell lysates were subjected to immunoprecipitation (IP) with anti-p73 antibody followed by IB with anti-p73 antibody. Actin expression served as a control for equal loading of proteins in each lane. *C*, FACS analysis. H1299 cells were transfected as in *A*. Forty-eight hours after transfection, attached and floating cells were harvested, stained with PI, and their cell cycle distributions examined by flow cytometry.

RNA Interference—To knock down the endogenous Plk1, H1299 cells were transiently transfected with the chemically synthesized siRNA targeting Plk1 or with the control siRNA (Dharmacon, Chicago) using Lipofectamine™ RNAiMAX (Invitrogen) according to the manufacturer's recommendations. Total RNA and whole cell lysates were prepared 48 h after transfection.

RESULTS

siRNA-mediated Knockdown of Plk1 Results in a Massive Apoptosis—To ask whether Plk1 could protect cells from p53-independent apoptosis, p53-deficient human lung carcinoma H1299 cells were transfected with control siRNA or with siRNA against Plk1. As shown in Fig. 1*A*, *Plk1* was successfully knocked down under our experimental conditions. The expression levels of *p73α* remained unchanged. Of note, the expression levels of pro-apoptotic $p53^{AIP1}$, which is one o the p53/p73 target genes, were significantly induced in Plk1-knocked down cells. Immunoblot analysis clearly demonstrated that the proteolytic cleavage of PARP, which is one of the substrates of the activated caspase-3 (30), is observed in Plk1-knocked down cells in association with a significant induction of pro-apoptotic p73α (Fig. 1*B*). FACS analysis revealed that siRNA-mediated knockdown of the endogenous Plk1 causes a remarkable increase in number of cells with sub-G_1 DNA content relative to control cells (Fig. 1*C*). Similar results were also obtained in H1299 cells transfected with other siRNAs against Plk1 (data not shown), suggesting that Plk1 might have an inhibitory effect on p73-mediated apoptosis. Similar results were also obtained

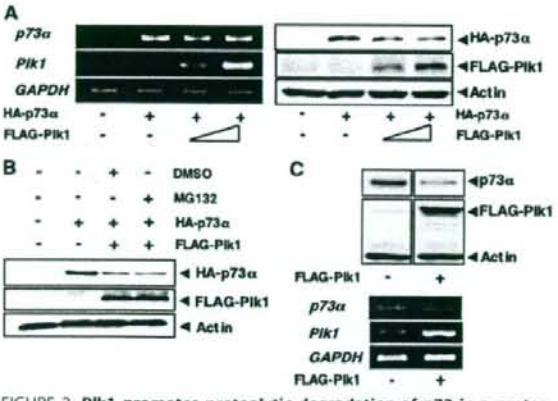

FIGURE 2. **Plk1 promotes proteolytic degradation of p73 in a proteasome-independent manner.** *A*, enforced expression of Plk1 reduces the expression levels of p73. H1299 cells were co-transfected with the constant amount of HA-p73α (0.5 μg) expression plasmid together with or without the expression plasmid for FLAG-Plk1 (0.5 and 1.0 μg). Forty-eight hours after transfection, total RNA and whole cell lysates were prepared and subjected to RT-PCR (*left panels*) and IB with the indicated antibodies (*right panels*), respectively. *B*, H1299 cells were transfected with the expression plasmid for HA-p73α alone or with HA-p73α (0.5 μg) plus FLAG-Plk1 (0.5 μg) expression plasmids. Forty-eight hours after transfection, cells were treated with *DMSO* or with 20 μM of MG-132 for 6 h. Whole cell lysates were then extracted and subjected to IB with the indicated antibodies. *C*, H1299 cells were transfected with pcDNA3 or with FLAG-Plk1 expression plasmid. Forty-eight hours after transfection, whole cell lysates and total RNA were prepared and subjected to IP with anti-p73 antibody followed by IB with anti-p73 antibody (*upper panels*) and RT-PCR (*lower panels*), respectively. Actin was used as a loading control, and *GAPDH* was used as an internal control.

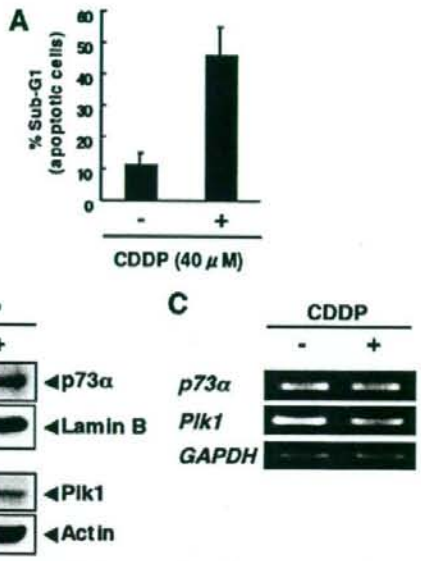

FIGURE 3. **Inverse relationship between the endogenous expression levels of p73 and Plk1 in response to CDDP.** *A–C*, COS7 cells were treated with 40 μM of CDDP or left untreated. Forty-eight hours after the treatment, floating and attached cells were collected, stained with PI, and their cell cycle distributions analyzed by flow cytometry (*A*). COS7 cells were treated with 40 μM of CDDP or left untreated. Forty-eight hours after the treatment, nuclear (*upper panels*) and whole cell lysates (*lower panels*) were prepared and subjected to IB with the indicated antibodies (*B*). Total RNA was also prepared and analyzed by RT-PCR (*C*).

in p53-proficient U2OS cells as well as p53-deficient SAOS-2 cells (supplemental Fig. S1). Thus, it is likely that siRNA-mediated knockdown of the endogenous Plk1 induces apoptosis regardless of *p53* status.

These findings showing that siRNA-mediated knockdown of Plk1 leads to a significant induction of the endogenous p73α at protein level prompted us to examine whether Plk1 could affect the protein stability of p73. For this purpose, H1299 cells were co-transfected with the constant amount of the expression plasmid for HA-p73α together with or without the increasing amounts of FLAG-Plk1 expression plasmid. As shown in Fig. 2*A*, *left panel*, Plk1 had undetectable effect on the expression levels of *p73α* mRNA. On the other hand, immunoblotting analysis revealed that Plk1 reduces the amounts of HA-p73α (Fig. 2*A*, *right panel*). Intriguingly, Plk1-mediated reduction of HA-p73α was not recovered in the presence of proteasome inhibitor MG-132 (Fig. 2*B*). Similar results were also obtained in cells exposed to lactacystin (data not shown). In addition, enforced expression of FLAG-Plk1 significantly reduced the amounts of the endogenous p73α at protein level but not at the mRNA level (Fig. 2*C*).

As described previously (31), CDDP treatment led to a stabilization of the endogenous p73α in COS7 cells, whereas the endogenous Plk1 was down-regulated in response to CDDP accompanied by the induction of apoptosis (Fig. 3, *A–C*), indicating that there exists an inverse relationship between the expression levels of Plk1 and p73α in response to CDDP and that Plk1 might promote proteolytic degradation of p73α in a proteasome-independent manner. Furthermore, enforced expression of Plk1 decreased the sensitivity to CDDP in association with the reduction of CDDP-mediated proteolytic cleavage of PARP (supplemental Fig. S2).

Plk1 Inhibits p73-mediated Transcriptional Activation and Pro-apoptotic Function—To address whether Plk1 could suppress the transcriptional activity of p73, we performed the luciferase reporter assays. H1299 cells were co-transfected with the constant amount of the expression plasmid for HA-p73α, the luciferase reporter construct carrying p53/p73-responsive $p21^{WAF1}$, *BAX*, or *MDM2* promoter, and *Renilla* luciferase cDNA (pRL-TK) together with or without the increasing amounts of FLAG-Plk1 expression plasmid. As shown in Fig. 4, *A–C*, enforced expression of FLAG-Plk1 significantly reduced the luciferase activities driven by the indicated promoters in a dose-dependent manner. Consistent with these results, HA-p73α-mediated up-regulation of the endogenous $p21^{WAF1}$, *BAX*, and *MDM2* mRNAs was abrogated by FLAG-Plk1 (Fig. 4*D*), suggesting that Plk1 has an ability to repress the transcriptional activity of p73α.

To examine a possible effect of Plk1 on pro-apoptotic activity of p73, we carried out apoptotic assay. H1299 cells were co-transfected with the indicated combinations of the expression plasmids. Consistent with the previous observations (32), HA-p73α alone increased number of cells with apoptotic nuclei (Fig. 5*A*). As expected, FLAG-Plk1 had an ability to decrease GFP-positive cells with apoptotic nuclei caused by exogenous expression of HA-p73α. In accordance with these results, FACS analysis demonstrated that HA-p73α-mediated increase in

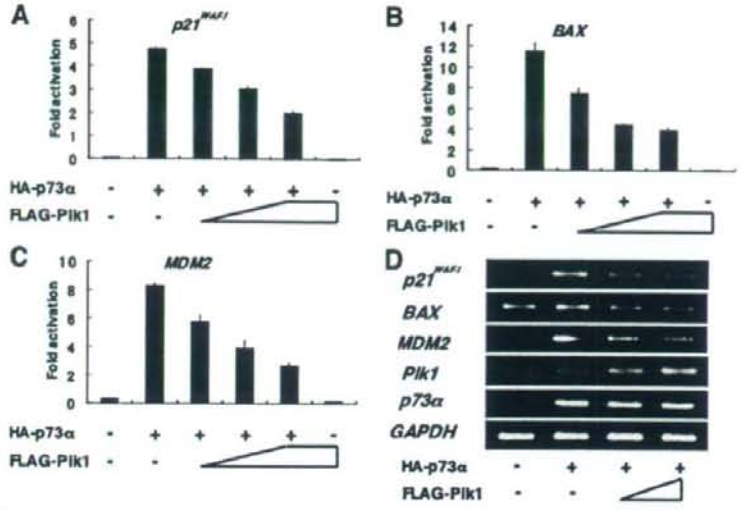

FIGURE 4. **Plk1 represses the p73-mediated transcriptional activation.** *A–C*, H1299 cells (5×10^4 cells) were co-transfected with the constant amount of HA-p73α expression plasmid (25 ng), 100 ng of p53/p73-responsive luciferase reporter construct bearing $p21^{WAF1}$ (*A*), *BAX* (*B*), or *MDM2* (C) promoter and 10 ng of *Renilla* luciferase reporter plasmid (pRL-TK) in the presence or absence of the increasing amounts of FLAG-Plk1 expression plasmid (50, 100, and 200 ng). To standardize the amounts of plasmid DNA per transfection, pcDNA3 was added to yield a total of 510 ng of plasmid. Forty-eight hours after transfection, cells were lysed, and their luciferase activities were measured. Data were normalized and presented as mean values ± S.D. of three independent experiments. *D*, RT-PCR analysis. H1299 cells were co-transfected with the constant amount of HA-p73α together with or without the increasing amounts of FLAG-Plk1 expression plasmid. Forty-eight hours after transfection, total RNA was prepared and analyzed for the expression levels of $p21^{WAF1}$, *BAX*, and *MDM2* by RT-PCR. Amplification of *GAPDH* serves as an internal control.

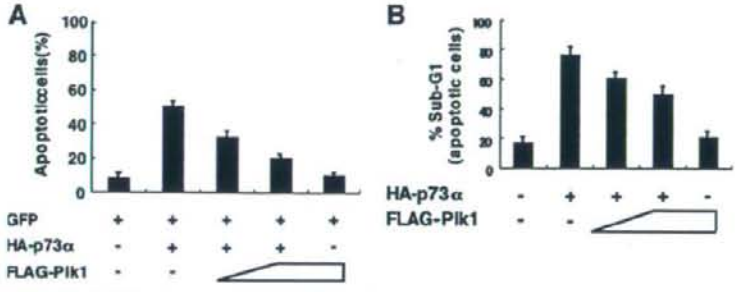

FIGURE 5. **Plk1 inhibits the pro-apoptotic activity of p73.** *A*, apoptotic assay. H1299 cells were seeded at a density of 2×10^5 cells/6-well tissue culture plate and allowed to attach overnight. Next day, cells were co-transfected with the constant amount of GFP (100 ng) and HA-p73α (900 ng) expression plasmids together with or without the increasing amounts of FLAG-Plk1 expression plasmid (500 and 1000 ng). Total amount of plasmid DNA was kept constant (2 μg) with pcDNA3. Forty-eight hours after transfection, cells were fixe, and cell nuclei were stained with DAPI. The percentages of GFP-positive cells with apoptotic nuclei were plotted. *B*, FACS analysis. H1299 cells were co-transfected with the constant amount of the expression plasmid encoding HA-p73α (250 ng) together with or without the increasing amounts of FLAG-Plk1 expression plasmid (100 or 200 ng). Forty-eight hours after transfection, attached and floating cells were collected, stained with PI, and their cell cycle distributions analyzed by flow cytometry.

number of cells with sub-G_1 DNA content is inhibited by co-expression with FLAG-Plk1 in a dose-dependent manner (Fig. 5*B*), indicating that Plk1 suppresses the p73α-mediated apoptotic cell death.

Interaction between Plk1 and p73 in Cells—To address whether Plk1 could associate with p73 in cells, we examined their subcellular distributions in response to CDDP. Human cervical carcinoma HeLa cells were treated with CDDP or left untreated for 24 h. Immunofluorescence microscopy demonstrated that the endogenous p73α is detectable in cell nucleus regardless of CDDP treatment (Fig. 6*A*). It was worth noting that the endogenous Plk1 localizes both in the cytoplasm and cell nucleus in the absence of CDDP, whereas CDDP treatment induces the nuclear accumulation of Plk1. Merged images revealed that Plk1 is largely co-localized with p73α in the cell nucleus in response to CDDP. Under our experimental conditions, immunofluorescence staining without primary antibodies did not show any positive signals (data not shown). These observations suggest that Plk1 might interact with p73 in cells exposed to CDDP.

To further confirm this notion, we performed immunoprecipitation experiments. HeLa cells were exposed to CDDP for 24 h, and whole cell lysates were immunoprecipitated with normal mouse serum (NMS) or with anti-p73 antibody followed by immunoblotting with anti-Plk1 antibody. As shown in Fig. 6*B*, *left panels*, the anti-p73 immunoprecipitates contained the endogenous Plk1. Reciprocal experiments demonstrated that p73 is co-immunoprecipitated with the endogenous Plk1 (Fig. 6*B*, *right panels*). Similar results were also obtained in the co-immunoprecipitation experiments using exogenous materials (supplemental Fig. S3). These observations strongly suggest that Plk1 interacts with p73α in cells.

To identify the essential region(s) of p73α required for the interaction with Plk1, we carried out *in vitro* pulldown assays. The indicated GST-p73α deletion mutants (Fig. 7*A*) were purified by glutathione-Sepharose beads (Fig. 7*B*). Each of these GST fusion proteins were incubated with the radiolabeled FLAG-Plk1, which was generated by *in vitro* transcription/translation system in the presence of [^{35}S]methionine. As clearly shown in Fig. 7*C*, the radiolabeled FLAG-Plk1 was efficiently pulled down by GST-p73α-(1–130) but not by the remaining GST fusion proteins, implying that the region between amino acid residues 63 and 113 of p73α is important for the interaction with Plk1.

In addition, we sought to determine the region of Plk1 required for the complex formation with p73α. To this end, we

generated the indicated Plk1 deletion mutants labeled with [^{35}S]methionine (Fig. 8*A*). These deletion mutants were incubated with GST-p73α-(1–130) (Fig. 8*B*). As shown in Fig. 8*C*, FLAG-Plk1-(1–401), FLAG-Plk1-(1–329), and FLAG-Plk1-(1–218) retained an ability to associate with GST-p73α-(1–130), whereas FLAG-Plk1-(1–98) failed to interact with GST-p73α-(1–130). These results indicated that the region between amino acid residues 99 and 218, including a part of the kinase domain of Plk1, is essential for the interaction with p73α.

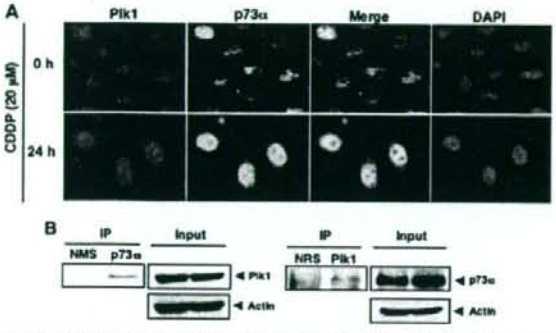

FIGURE 6. **Interaction between Plk1 and p73 in cells.** *A*, nuclear co-localization of Plk1 with p73 in response to CDDP. HeLa cells were treated with 20 μM CDDP (*lower panels*) or left untreated (*upper panels*). Twenty-four hours after the treatment cells were simultaneously probed with polyclonal anti-p73 antibody and monoclonal anti-Plk1 antibody for 1 h at room temperature. After extensive washing in PBS, cells were incubated with rhodamine-conjugated anti-mouse IgG (*red*) and fluorescein isothiocyanate-conjugated anti-rabbit IgG (*green*). Cell nuclei were stained with DAPI (*blue*). Merged images indicate the nuclear co-localization of Plk1 with p73α (*yellow*). *B*, immunoprecipitation. HeLa cells were exposed to 20 μM CDDP. Twenty-four hours after CDDP treatment, whole cell lysates were IP with NMS or with anti-p73 antibody followed by IB with anti-Plk1 antibody (*left panel*). Input lysates were analyzed by IB with the indicated antibodies. Reciprocal experiments are shown in the *right panels*.

Kinase Activity of Plk1 Is Required for the Inhibition of p73 Function—To examine whether the kinase activity of Plk1 could be necessary for the inhibition of p73 function, we tested a possible effect of the kinase-deficient mutant form of Plk1 (Plk1(K82M)) (20) on p73α. For this purpose, we first examined whether Plk1(K82M) could interact with p73α in cells. COS7 cells were co-transfected with the expression plasmids encoding HA-p73α and FLAG-Plk1(K82M). Forty-eight hours after transfection, whole cell lysates were immunoprecipitated with NMS or with anti-FLAG antibody followed by immunoblotting with anti-p73 or with anti-FLAG antibody. As seen in Fig. 9*A*, *left panels*, HA-p73α was co-immunoprecipitated with FLAG-Plk1(K82M). Similarly, the anti-p73 immunoprecipitates contained FLAG-Plk1(K82M) (Fig. 9*A*, *right panels*). These results suggest that the kinase-deficient mutant form of Plk1 retains an ability to interact with p73 in cells.

To further examine the effect of the kinase activity of Plk1 on p73 function, we performed luciferase reporter assays. H1299 cells were co-transfected with the constant amount of the expression plasmid for HA-p73α, luciferase reporter construct bearing p53/p73-responsive *p21^{WAF1}*, *BAX*, or *MDM2* promoter, and *Renilla* luciferase cDNA along with or without the increasing amounts of FLAG-Plk1(K82M). As shown in Fig. 9, *B–D*, FLAG-Plk1(K82M) had negligible effect on the transcriptional activity of HA-p73α. In contrast to wild-type Plk1, enforced expression of FLAG-Plk1(K82M) in H1299 cells had marginal effect on the expression levels of the endogenous p73α (supplemental Fig. S4). Collectively, these results indicate that kinase activity of Plk1 is required for the inhibition of p73 function.

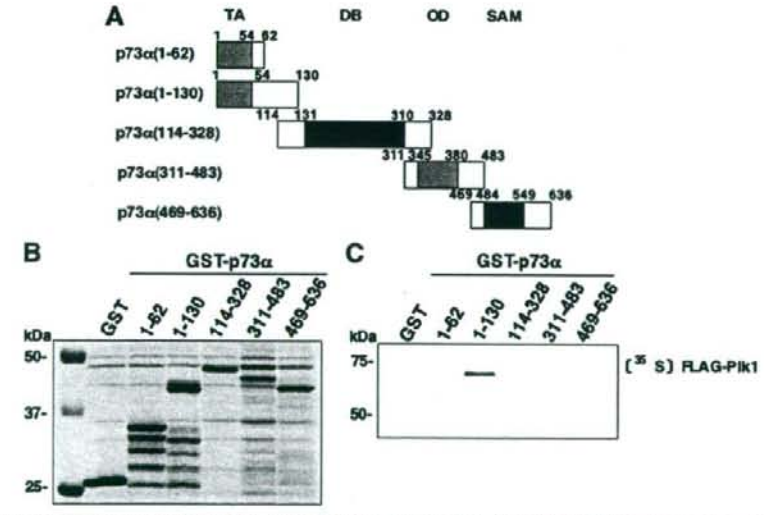

FIGURE 7. **NH_2-terminal small domain of p73 is required for the interaction with Plk1.** *A*, domain structure of wild-type p73α and schematic representation of GST-tagged p73α deletion mutants. *TA*, transactivation domain; *DB*, DNA-binding domain; *OD*, oligomerization domain; *SAM*, sterile α-motif domain. *Numbers* indicate amino acid positions. *B*, GST and GST-p73α fusion proteins were purified by glutathione-Sepharose beads and separated by 10% SDS-PAGE followed by Coomassie Brilliant Blue staining. *C*, *in vitro* pulldown assay. Equal amount of radiolabeled FLAG-Plk1 was incubated with GST or with the indicated GST-p73α fusion proteins. After incubation, GST or GST-p73α fusion proteins were recovered by glutathione-Sepharose beads, and bound materials were resolved by 10% SDS-PAGE followed by autoradiography.

Plk1 Phosphorylates p73 in Vitro—To address whether Plk1 could phosphorylate p73, we performed *in vitro* kinase reaction (29). To this end, we employed a CycLex Plk1 assay kit. As a positive control, we used protein X, which was provided by the manufacturer. According to the manufacturer's instructions, the active form of Plk1 was incubated with anti-phospho-Thr antibody, and then substrate proteins, including protein X, GST, or the indicated GST-p73α fusion proteins (Fig. 10*A*) were added to the reaction mixture. After the incubation, horseradish peroxidase-conjugated secondary antibody was mixed with the reaction mixtures. As shown in Fig. 10*B*, *yellow* color was observed in the reaction mixtures containing protein X, GST-p73α-(1–62), and GST-p73α-(1–130). Fig. 10*C* shows the results of quantification of the reactions, suggesting that Plk1 might phosphorylate Thr residue(s)

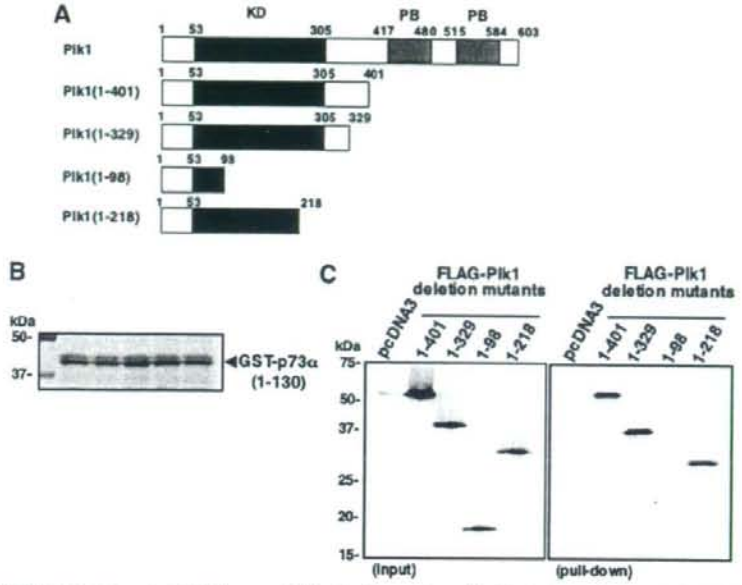

FIGURE 8. **Kinase domain of Plk1 is essential for the interaction with p73.** *A*, schematic drawing of wild-type Plk1 and its deletion mutants. *KD*, kinase domain; *PB*, polo-box domain. *B*, Coomassie Brilliant Blue staining of GST-p73α-(1–130) used for this study. *C*, *in vitro* pulldown assay. Equal amount of GST-p73α-(1–130) was incubated with radiolabeled FLAG-Plk1 deletion mutants (*left panel*). After incubation, GST-p73α-(1–130) was precipitated by glutathione-Sepharose beads, and bound materials were separated by SDS-PAGE followed by autoradiography.

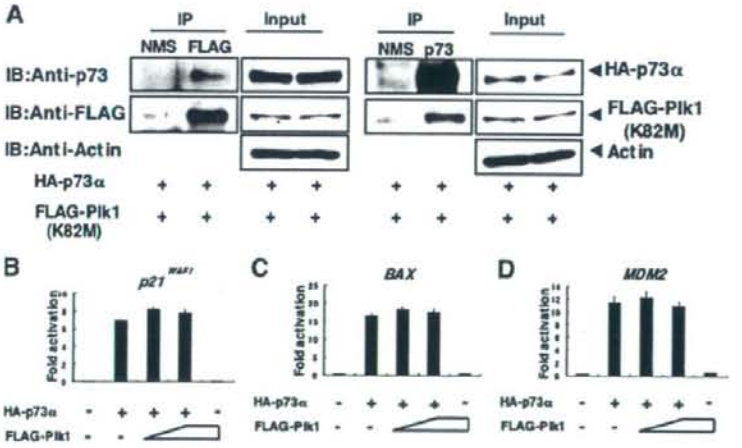

FIGURE 9. **Kinase activity of Plk1 is required for the inhibition of p73.** *A*, Plk1(K82M) retains an ability to interact with p73 in cells. COS7 cells were transiently co-transfected with the expression plasmids for HA-p73α and FLAG-Plk1(K82M). Forty-eight hours after transfection, whole cell lysates were prepared and subjected to IP with NMS or with anti-FLAG antibody. The immunoprecipitates were analyzed by IB with anti-p73 (*1st panel*) or with anti-FLAG (*2nd panel*) antibody. Input lysates were processed for IB with the indicated antibodies. *Right panels* show the results of the reciprocal experiments. *B–D*, luciferase reporter assay. H1299 cells were transiently co-transfected with the constant amount of HA-p73α expression plasmid (25 ng), 100 ng of luciferase reporter construct carrying p53/p73-responsive element derived from $p21^{WAF1}$ (*B*), *Bax* (*C*), or *MDM2* (*D*) promoter and 10 ng of pRL-TK together with or without the increasing amounts of the expression plasmid for FLAG-Plk1(K82M) (50 and 100 ng). Forty-eight hours after transfection, cells were lysed and their luciferase activities determined. Firefly luminescence signal was normalized based on the *Renilla* luminescence signal. Results were shown as fold induction of the firefly luciferase activity compared with control cells transfected with the empty plasmid alone.

within the region between amino acid residues 1 and 130 of p73α.

As described previously (33), a sequence (D/E)*X*(S/T)ψ*X*(D/E) (where *X* is any amino acid; ψ is hydrophobic amino acid) was identified as a consensus motif for Plk1-dependent phosphorylation. During the search for a putative phosphorylation site(s) targeted by Plk1 within the amino acid sequence of p73α (residues 1–130), we found out a related motif (^{25}DSTYFD^{30}) was in the NH_2-terminal portion of p73α. To further confirm whether Thr-27 of p73α could be phosphorylated by Plk1, we generated a mutant form of GST-p73α-(1–130), termed T27A, where Thr-27 was substituted to Ala. Purified GST fusion proteins (Fig. 11*A*) were subjected to the *in vitro* kinase reaction. As shown in Fig. 11, *B* and *C*, the amino acid substitution resulted in a significant reduction of Plk1-mediated phosphorylation level of GST-p73α-(1–130). Consistent with these results, GST-p73α-(1–130) and S48A mutant were strongly radiolabeled in the presence of Plk1, whereas T27A mutant was labeled to a lesser degree (Fig. 11*D*), indicating that Thr-27 of p73α is at least one of the phosphorylation sites targeted by Plk1. Taken together, our current results have exposed a novel molecular mechanism behind Plk1-mediated protection of cells from p73-dependent apoptosis.

DISCUSSION

In this study, we have found for the first time that p73 plays a crucial role in the induction of massive apoptosis in p53-deficient cells caused by siRNA-mediated depletion of the endogenous Plk1. Thus, it is likely that Plk1 protects p53-deficient cells from p73-mediated apoptosis. In this connection, inhibition of Plk1 function might provide a novel therapeutic strategy to treat tumors with *p53* mutation.

We have previously demonstrated that Plk1 interacts with p53 and suppresses its transcriptional as well as pro-apoptotic activity (20). According to our previous results,

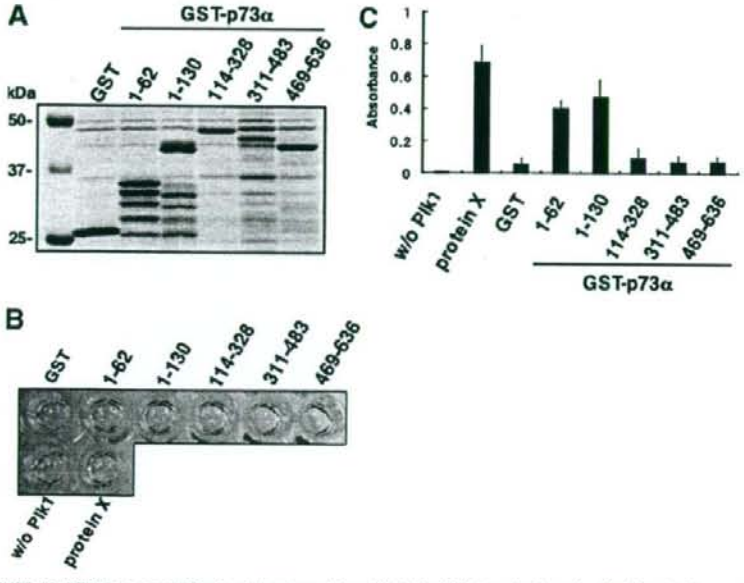

FIGURE 10. **Plk1 has an ability to phosphorylate p73 at its NH_2-terminal region *in vitro*.** *A*, Coomassie Brilliant Blue staining of GST or GST-p73α fusion proteins used for *in vitro* kinase reaction. *B*, *in vitro* kinase assay. GST or the indicated GST-p73α deletion mutants bound to glutathione-Sepharose beads were washed with washing buffer and resuspended in 90 μl of kinase reaction buffer. Protein X, which was supplied by manufacturer, was used as a positive control. 10 μl of the active form of Plk1 were added to the reaction mixtures and incubated at 30 °C for 30 min. The reaction mixtures were washed with washing buffer and then incubated with 100 μl of polyclonal anti-phospho-Thr antibody at room temperature for 30 min followed by incubation with horseradish peroxidase-conjugated anti-rabbit IgG at room temperature for 30 min. After incubation, 100 μl of substrate reagent were added to the reaction mixtures and incubated at room temperature for 5 min. *Yellow* coloration indicates the Plk1-mediated phosphorylation at Thr residue. After the addition of 100 μl of stop solution, supernatant was transferred into 96-well tissue culture plate, and the absorbance reading was carried out at 450/540 nm using the microplate reader (*C*).

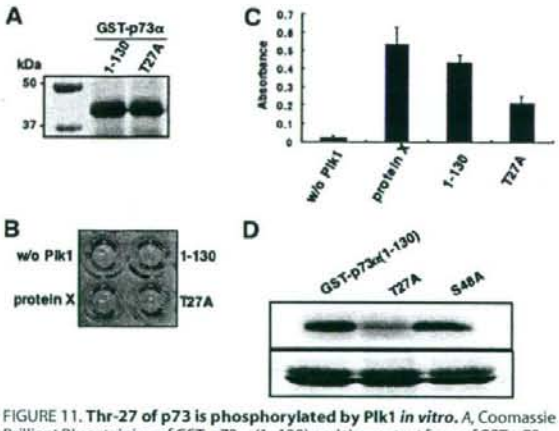

FIGURE 11. **Thr-27 of p73 is phosphorylated by Plk1 *in vitro*.** *A*, Coomassie Brilliant Blue staining of GST-p73α-(1–130) and the mutant form of GST-p73α-(1–130) termed T27A where Thr-27 was substituted to Ala. *B*, *in vitro* kinase assay. *In vitro* kinase reactions were performed using GST-p73α-(1–130) and T27A as described in Fig. 10*B*. *C*, absorbance reading of the *in vitro* kinase reactions. *D*, standard *in vitro* kinase assay. GST-p73α-(1–130), T27A, and S48A were incubated with the active form of Plk1 in the presence of [γ-^{32}P]ATP. The reaction mixtures were separated by SDS-PAGE and subjected to autoradiography (*top panel*). *Bottom panel* showed the Coomassie Brilliant Blue staining of the GST-p73α fusion proteins.

Plk1 bound to a DNA-binding domain of p53 and inhibited its transcriptional activity. For p73, Plk1 interacted with the region between NH_2-terminal transactivation domain and a DNA-binding domain of p73α, which includes the proline-rich domain (amino acid residues 81–113). Because NH_2-terminal proline-rich domain is involved in the transcriptional activity of p73 (34), it is possible that Plk1 masks the proline-rich domain to render p73α latent form. Thus, it is likely that Plk1-mediated inhibitory mechanisms of p73 is distinct from those of p53.

In response to CDDP, p73α as well as p53 is induced to accumulate in association with a down-regulation of Plk1 (20). Under our experimental conditions, Plk1 has an ability to promote a proteolytic degradation of p73 in a proteasome-independent manner. As described (35), calpain promoted the proteolytic cleavage of p73. However, our preliminary experiments demonstrated that the calpain inhibitor had an undetectable effect on Plk1-mediated proteolytic degradation of p73 (data not shown). Although the precise molecular mechanisms behind the Plk1-mediated proteolytic degradation of p73 remain unclear, our present results indicate that, under normal conditions, Plk1 might contribute to maintain pro-apoptotic p73 at extremely low levels and also suggest that Plk1-mediated proteolytic degradation of p73α might be an alternative molecular mechanism of p73 dysfunction. Similarly, Liu and Erikson (25) described that Plk1 depletion stabilizes p53 in HeLa cells. In support with this notion, Chen *et al.* (36) found that Plk1 inhibits UV-mediated phosphorylation of p53 at Ser-15 and thereby facilitates its nuclear export and proteolytic degradation.

As described (2, 3), p73 function is modulated by post-translational modifications such as phosphorylation and acetylation. Several lines of evidence suggest that phosphorylation of p73 does not always enhance its function (8–13). Based on our present results, Plk1 inhibited the p73α-mediated transcriptional activation, whereas the kinase-deficient mutant form of Plk1 did not, indicating that Plk1-dependent phosphorylation of p73 plays an inhibitory role in the regulation of p73 activity. In accordance with this notion, our *in vitro* kinase reactions demonstrated that GST-p73α-(1–130) is phosphorylated by Plk1. During the extensive search for putative phosphorylation site(s) within the NH_2-terminal portion of p73α, we found out two canonical phosphorylation sites targeted by Plk1, including (^{25}DSTYFD^{30}) and (^{46}DSSMDV^{51}). Thr-27 substituted to Ala

(T27A) resulted in a significant reduction of Plk1-mediated phosphorylation of GST-p73α-(1–130), whereas S48A mutant was efficiently phosphorylated by Plk1, suggesting that Thr-27 is at least one of the phosphorylation site(s) of p73α. Considering that Thr-27 exists within the transactivation domain of p73, it is likely that Plk1-mediated phosphorylation of p73α at Thr-27 might induce the conformational change of its transactivation domain and/or the dissociation of the co-activator such as p300/CBP from p73α, and thereby inhibiting transcriptional as well as pro-apoptotic activity of p73α. Indeed, Plk1 inhibited the complex formation between p73 and p300 (supplemental Fig. S5). In addition, it has been shown that p300-mediated acetylation of p73 increases the stability of p73 (15). Thus, it is possible that Plk1-mediated phosphorylation of p73 inhibits p73 function through the dissociation of p300 from p73 and also induces the degradation of latent forms of p73. Further studies should be required to address this issue.

Another finding of this study was that the endogenous Plk1 begins to accumulate in the cell nucleus in response to CDDP treatment. Based on our present results, Plk1 interacts with p73 and inhibits the apoptosis mediated by p73. Because the expression levels of Plk1 decreased in cells exposed to CDDP, p73 might be liberated from the inhibitory complex containing Plk1 to exert its pro-apoptotic activity. The precise molecular mechanisms behind the CDDP-induced nuclear accumulation of Plk1 remain unclear.

It has been well documented that the elevated levels of Plk1 expression show various human tumors (21, 37), and patients with tumors showed a clear correlation between lower survival rates and higher Plk1 expression levels (37–39). Taken together with our present and previous results (20), Plk1 has an ability to block the p53- and p73-dependent pro-apoptotic pathway, raising the possibility that Plk1 is one of the potential targets in cancer treatment.

Acknowledgment—We thank Y. Nakamura for technical assistance.

REFERENCES

1. Kaghad, M., Bonnet, H., Yang, A., Creancier, L., Biscan, J. C., Valent, A., Minty, A., Chalon, P., Lelias, J. M., Dumont, X., Ferrara, P., McKeon, F., and Caput, D. (1997) *Cell* **90,** 809–819
2. Melino, G., De Laurenzi, V., and Vousden, K. H. (2002) *Nat. Rev. Cancer* **2,** 605–615
3. Ozaki, T., and Nakagawara, A. (2005) *Cancer Sci.* **96,** 729–737
4. Bourdon, J. C., Fernandes, K., Murray-Zmijewski, F., Liu, G., Diot, A., Xirodiamas, D. P., Saville, M. K., and Lane, D. P. (2005) *Genes Dev.* **19,** 2122–2137
5. Stiewe, T., Zimmermann, S., Frilling, A., Esche, H., and Putzer, B. M. (2002) *Cancer Res.* **62,** 3598–3602
6. Pozniak, C. D., Radinovic, S., Yang, A., McKeon, F., Kaplan, D. R., and Miller, F. D. (2000) *Science* **289,** 304–306
7. Irwin, M., Kondo, K., Marin, M. C., Cheng, L. S., Hahn, W. C., and Kaelin, W. G., Jr. (2003) *Cancer Cell* **3,** 403–410
8. Gong, J., Costanzo, A., Yang, H.-Q., Melino, G., Kaelin, W. G., Jr., Levreno, M., and Wang, J. Y. (1999) *Nature* **399,** 806–809
9. Agami, R., Blandino, G., Oren, M., and Shaul, Y. (1999) *Nature* **399,** 809–813
10. Yuan, Z.-M., Shioya, H., Ishiko, T., Sun, X., Gu, J., Huang, Y. Y., Lu, H., Kharbanda, S., Weichselbaum, R., and Kufe, D. (1999) *Nature* **399,** 814–817
11. Ren, J., Datta, R., Shioya, H., Li, Y., Oki, E., Biedermann, V., Bharti, A., and Kufe, D. (2002) *J. Biol. Chem.* **277,** 33758–33765
12. Gonzalez, S., Prives, C., and Cordon-Cordo, C. (2003) *Mol. Cell. Biol.* **23,** 8161–8171
13. Gaiddon, C., Lokshin, M., Gross, I., Levasseur, D., Taya, Y., Loeffler, J.-P., and Prives, C. (2003) *J. Biol. Chem.* **278,** 27421–27431
14. Zeng, X., Li, X., Miller, A., Yuan, Z., Yuan, W., Kwok, R. P., Goodman, R., and Lu, H. (2000) *Mol. Cell. Biol.* **20,** 1299–1310
15. Costanzo, A., Merlo, P., Pediconi, N., Fulco, M., Sartorelli, V., Cole, P. A., Fontemaggi, G., Fanciulli, M., Schiltz, L., Blandino, G., Balsano, C., and Levrero, M. (2002) *Mol. Cell* **9,** 175–186
16. Barr, F. A., Sillje, H. H., and Nigg, E. A. (2004) *Nat. Rev. Mol. Cell Biol.* **5,** 429–440
17. Xie, S. Xie, B., Lee, M. Y., and Dai, W. (2005) *Oncogene* **24,** 277–286
18. Dai, W. (2005) *Oncogene* **24,** 214–216
19. Elia, A. E., Cantley, L. C., and Yaffe, M. B. (2003) *Science* **299,** 1228–1231
20. Ando, K., Ozaki, T., Yamamoto, H., Furuya, K., Hosoda, M., Hayashi, S., Fukuzawa, M., and Nakagawara, A. (2004) *J. Biol. Chem.* **279,** 25549–25561
21. Eckerdt, F., Yuan, J., and Strebhardt, K. (2005) *Oncogene* **24,** 267–276
22. Smith, M. R., Wilson, M. L., Hamanaka, R., Chase, D., Kung, H., Longo, D. L., and Ferris, D. K. (1997) *Biochem. Biophys. Res. Commun.* **234,** 397–405
23. Spankuch-Schmitt, B., Bereiter-Hahn, J., Kaufmann, M., and Strebhardt, K. (2002) *J. Natl. Cancer Inst.* **94,** 1863–1877
24. Spankuch-Schmitt, B., Wolf, G., Solbach, C., Loibl, S., Knecht, R., Stegmuller, M., von Minckwitz, G., Kaufmann, M., and Strebhardt, K. (2002) *Oncogene* **21,** 3162–3171
25. Liu, X., and Erikson, R. L. (2003) *Proc. Natl. Acad. Sci. U. S. A.* **100,** 5789–5794
26. Smits, V. A., Klompmaker, R., Arnaud, L., Rijksen, G., Nigg, E. A., and Medema, R. H. (2000) *Nat. Cell Biol.* **2,** 672–676
27. van Vugt, M. A., Smits, V. A., Klompmaker, R., Medema, R. H. (2001) *J. Biol. Chem.* **276,** 41656–41660
28. Liu, X., Lei, M., and Erikson, R. L. (2006) *Mol. Cell. Biol.* **26,** 2093–2108
29. Liu, Y., Shreder, K. R., Gai, W., Corral, S., Ferris, D. K., and Rosenblum, J. S. (2005) *Chem. Biol.* **12,** 99–107
30. Niizuma, T., Nakamura, Y., Ozaki, T., Nakanishi, H., Ohira, M., Isogai, E., Kageyama, H., Imaizumi, M., and Nakagawara, A. (2006) *Oncogene* **26,** 5046–5055
31. Hosoda, M., Ozaki, T., Miyazaki, K., Hayashi, S., Furuya, K., Watanabe, K., Nakagawa, T., Hanamoto, T., Todo, S., and Nakagawara, A. (2005) *Oncogene* **24,** 7156–7169
32. Zeng, X., Chen, L., Jost, C. A., Maya, R., Keller, D., Wang, X., Kaelin, W. G., Jr., Oren, M., Chen, J., and Lu, H. (1999) *Mol. Cell. Biol.* **19,** 3257–3266
33. Nakajima, H., Toyoshima-Morimoto, F., Taniguchi, E., and Nishida, E. (2003) *J. Biol. Chem.* **278,** 25277–25280
34. Tanaka, Y., Kameoka, M., Itaya, A., Ota, K., and Yoshihara, K. (2004) *Biochem. Biophys. Res. Commun.* **317,** 865–872
35. Munarriz, E., Bano, D., Sayan, A. E., Rossi, M., Melino, G., and Nicotera, P. (2005) *Biochem. Biophys. Res. Commun.* **333,** 954–960
36. Chen, J., Dai, G., Wang, Y. Q., Wang, S., Pan, F. Y., Xue, B., Zhao, D. H., and Li, C. J. (2006) *FEBS Lett.* **580,** 3624–3630
37. Takai, N., Hamanaka, R., Yoshimatsu, J., and Miyakawa, Y. (2005) *Oncogene* **24,** 287–291
38. Knecht, R., Elez, R., Oechler, M., Solbach, C., von Ilberg, C., and Strebhardt, K. (1999) *Cancer Res.* **59,** 2794–2797
39. Knecht, R., Oberhauser, C., and Strebhardt, K. (2000) *Int. J. Cancer* **89,** 535–536

Oncogene (2008) 27, 6075–6082

www.nature.com/onc

SHORT COMMUNICATION

N-MYC promotes cell proliferation through a direct transactivation of neuronal leucine-rich repeat protein-1 (*NLRR1*) gene in neuroblastoma

MS Hossain[1,2,5], T Ozaki[1,2,5], H Wang[1,3,5], A Nakagawa[4], H Takenobu[1], M Ohira[1], T Kamijo[1] and A Nakagawara[1,2]

[1]*Division of Biochemistry, Chiba Cancer Center Research Institute, Chiba, Japan;* [2]*Department of Molecular Biology and Oncology, Chiba University Graduate School of Medicine, Chiba, Japan;* [3]*Department of Pediatrics, ShengJing Hospital of China Medical University, Shenyang, People's Republic of China and* [4]*Department of Pathology, National Center for Child Health and Development, Tokyo, Japan*

Neuronal leucine-rich repeat protein-1 (*NLRR1*) gene encodes a type I transmembrane protein with unknown function. We have previously described that *NLRR1* gene is highly expressed in unfavorable neuroblastomas as compared with favorable tumors and its higher expression levels correlate significantly with poor clinical outcome. In this study, we have found that *NLRR1* gene is one of direct target genes for N-MYC and its gene product contributes to N-MYC-dependent growth promotion in neuroblastoma. Expression levels of *NLRR1* were significantly associated with those of N-*MYC* in various neuroblastoma cell lines as well as primary neuroblastoma tissues. Indeed, enforced expression of N-MYC resulted in a remarkable induction of the endogenous *NLRR1*. Consistent with these results, we have identified two functional E-boxes within the promoter region and intron 1 of *NLRR1* gene. Intriguingly, c-myc also transactivated *NLRR1* gene. Enforced expression of NLRR1 promoted cell proliferation and rendered cells resistant to serum deprivation. In support with these observations, small-interfering RNA-mediated knockdown of the endogenous *NLRR1*-reduced growth rate and sensitized cells to serum starvation. Collectively, our present findings provide a novel insight into understanding molecular mechanisms behind aggressive neuroblastoma with N-*MYC* amplification.
Oncogene (2008) **27**, 6075–6082; doi:10.1038/onc.2008.200; published online 30 June 2008

Keywords: c-myc; neuroblastoma; N-MYC; NLRR1; proliferation; transactivation

In a sharp contrast to c-*myc*, the expression of N-*MYC* is largely restricted to embryonic tissues and neuroendocrine tumors (Boon *et al.*, 2001). It has been established that N-*MYC* gene amplification is strongly associated with poor clinical outcome of aggressive human neuroblastoma (Kohl *et al.*, 1983; Schwab *et al.*, 1983; Seeger *et al.*, 1985). Indeed, enforced expression of N-*MYC* in neuroblastoma cell lines resulted in an accelerated proliferation (Bernards *et al.*, 1986; Lutz *et al.*, 1996), whereas treatment of neuroblastoma cells with antisense oligonucleotides specific to N-*MYC* decreased their proliferation (Negroni *et al.*, 1991). Consistent with these observations, transgenic mice overexpressing N-*MYC* in neural crest-derived tissues displayed frequent development of neuroblastomas (Weiss *et al.*, 1997), suggesting that deregulated expression of N-MYC is causative in genesis and development of neuroblastoma *in vivo*. However, it is still unclear how N-MYC contributes to the formation of neoplastic phenotypes of neuroblastoma.

N-MYC is a nuclear transcription factor containing NH_2-terminal transactivation domain and COOH-terminal helix-loop-helix/leucine-zipper domain as well as the basic region (Kouzarides and Ziff, 1988; Landschulz *et al.*, 1988; Murre *et al.*, 1989). N-MYC forms a heterodimeric complex with Max through their helix-loop-helix/leucine-zipper domains and binds to consensus site known as E-box (CACGTG) (Alex *et al.*, 1992; Blackwood *et al.*, 1992; Torres *et al.*, 1992). Identification of its direct transcriptional target gene(s) might provide a novel insight into understanding the functional contribution of N-MYC in malignant phenotypes of aggressive neuroblastoma. Extensive efforts demonstrated that prothymosin-α, ornithine decarboxylase teromerase reverse transcriptase, *Id2* and genes involved in ribosome biogenesis are transcriptional targets of N-MYC (Lutz *et al.*, 1996; Wang *et al.*, 1998; Lasorella *et al.*, 2000; Boon *et al.*, 2001). Recently, Slack *et al.* (2005) described that MDM2 that acts as an E3 ubiquitin protein ligase for tumor suppressor, p53, is a putative transcriptional target of N-MYC. According to their results, N-MYC directly binds to a consensus E-box within human *MDM2* promoter region and N-MYC has an ability to transactivate *MDM2* promoter. Furthermore, the endogenous MDM2 increased in N-MYC-inducible neuroblastoma cells. These observations suggest that MDM2 is important in N-MYC-driven neuroblastoma development.

Correspondence: Dr A Nakagawara, Division of Biochemistry, Chiba Cancer Center Research Institute, 666-2 Nitona, Chuoh-ku, Chiba 260-8717, Japan.
E-mail: akiranak@chiba-cc.jp
[5]These authors contributed equally to this work.
Received 28 February 2008; revised 30 April 2008; accepted 22 May 2008; published online 30 June 2008

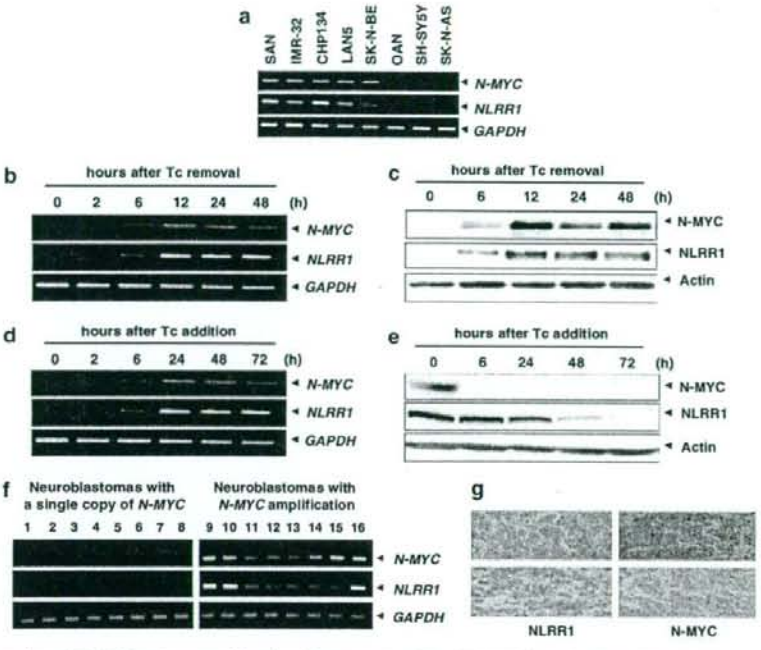

Figure 1 Expression of N-*MYC* and neuronal leucine-rich repeat protein-1 (*NLRR1*) in various neuroblastoma-derived cell lines and primary tissues. (**a**) Expression of *NLRR1* is restricted in neuroblastoma cell lines with N-*MYC* amplification. Total RNA was prepared from neuroblastoma cell lines with N-*MYC* amplification (SAN, IMR-32, CHP134, LAN5 and SK-N-BE) and neuroblastoma cell lines bearing a single copy of N-*MYC* (OAN, SH-SY5Y and SK-N-AS) using RNeasy Mini Kit (Qiagen, Valencia, CA, USA) and analysed for expression levels of N-*MYC* (top) and *NLRR1* (middle) by reverse transcription (RT) PCR. *GAPDH* was used as an internal control (bottom) The oligonucleotide primer sequences used in this study are as follows: human *NLRR1*, 5′-GTCGATGTCCATGAATACAACCT-3′ (sense) and 5′-CAAGGCTAATGACGGCAAAC-3′ (antisense); human *N-MYC*, 5′-CTTCGGTCCAGCTTTCTCAC-3′ (sense) and 5′-GTCCGAGCGTGTTCAATTTT-3′ (antisense); human *GAPDH*, 5′-ACCTGACCTGCCGTCTAGAA-3′ (sense) and 5′-TCCACCACCCTGTTGCTGTA-3′ (antisense). (**b**, **c**) Induction of NLRR1 in N-*MYC*-inducible Tet21N cells. At the indicated time points after removal of tetracycline (Tc), total RNA and cell lysates were prepared and processed for RT PCR (**b**) and immunoblotting with anti-N-MYC (Ab-1, Oncogene Research Products, Cambridge, MA, USA), anti-NLRR1 and anti-actin (20 33, Sigma, St Louis, MO, USA) antibodies (**c**), respectively. For RT PCR, *GAPDH* was used as an internal control. For immunoblotting, actin was used as a loading control. (**d**, **e**) Downregulation of NLRR1 in Tet21N cells maintained in the presence of Tc. At the indicated time periods after the addition of Tc (100 ng/ml), total RNA and cell lysates were prepared and subjected to RT PCR (**d**) and immunoblotting (**e**), respectively. (**f**) Expression of *NLRR1* in primary neuroblastomas. Total RNA was prepared from eight favorable neuroblastomas (cases 1 8) and eight unfavorable ones (cases 9 16) and subjected to RT PCR to examine expression levels of N-*MYC* (top) and *NLRR1* (middle). *GAPDH* was used as an internal control (bottom). (**g**) Immunohistochemical analysis. Primary neuroblastomas tissues with *N-MYC* amplification were immunostained with anti-NLRR1 (left panels) or with anti-N-MYC antibody (right panels). The BenchMark XT immunostainer (Ventana Medical Systems, Tucson, AZ, USA) and 3,3′ diaminobenzidine detection kit (Ventana Medical Systems) were used to visualize NLRR1 and N-MYC. All patients agreed to participate and provided written informed consent and our present study was approved by institutional ethical review committee.

Mammalian neuronal leucine-rich repeat protein family (NLRR) is a type I transmembrane protein with extracellular leucine-rich repeats, which is composed of NLRR1-5 (Taguchi *et al*., 1996; Taniguchi *et al*., 1996; Hamano *et al*., 2004; Bando *et al*., 2005). NLRR proteins have been proposed to function as cell adhesion or signaling molecules (Fukamachi *et al*., 2002). We have previously reported that expression levels of *NLRR1* are significantly higher in unfavorable neuroblastoma than those in favorable one and higher expression levels of *NLRR1* closely correlate with poor clinical outcome of patients with neuroblastoma (Hamano *et al*., 2004). In contrast, *NLRR3* and *NLRR5* were expressed at higher levels in favorable neuroblastoma as compared with unfavorable one. For *NLRR2*, no significant differences were observed in its expression levels between favorable and unfavorable neuroblastomas (Hamano *et al*., 2004). In the present study, we have found that *NLRR1* is a direct transcriptional target of N-MYC and its gene product is important in the regulation of neuroblastoma cell proliferation.

To examine a possible correlation between expression levels of N-*MYC* and *NLRR1* in neuroblastoma cells, total RNA was prepared from the indicated cell lines and subjected to reverse transcription (RT)–PCR. As shown in Figure 1a, all neuroblastoma cell lines

with N-*MYC* amplification that we examined expressed *NLRR1* mRNA, whereas we did not detect *NLRR1* mRNA in OAN, SH-SY5Y and SK-N-AS cells bearing a single copy of N-*MYC* under our experimental conditions. To confirm a possible relationship between N-*MYC* and *NLRR1*, we employed N-*MYC*-inducible neuroblastoma cells (Tet21N) derived from parental neuroblastoma cell line SHEP (Lutz *et al*., 1996). According to their results, Tet21N cells constitutively expressed N-*MYC* in the absence of tetracycline (Tc), whereas the addition of Tc to the culture decreased N-*MYC* expression levels. For this purpose, we have generated polyclonal antibody against NLRR1 that recognizes the region including amino-acid residues between positions 693 and 712. At the indicated time points after Tc depletion, total RNA and cell lysates were prepared and subjected to RT–PCR and immunoblotting, respectively. As shown in Figure 1b, Tc deprivation led to an induction of N-*MYC* in association with a significant increase in expression levels of *NLRR1*. Similar results were also obtained in immunoblotting analysis (Figure 1c). In contrast to the withdrawal of Tc, the addition of Tc to the culture significantly reduced expression levels of N-*MYC* and the concomitant decrease in expression levels of *NLRR1* was detectable at mRNA and protein levels (Figures 1d and e), suggesting that *NLRR1* might be a direct transcriptional target of N-MYC.

Consistent with these results, *NLRR1* expression was undetectable in favorable primary neuroblastomas carrying a single copy of N-*MYC*, whereas unfavorable primary neuroblastomas bearing N-*MYC* amplification expressed substantial amounts of *NLRR1* (Figure 1f). Immunohistochemical analyses also revealed that NLRR1 is coexpressed with N-MYC in primary neuroblastomas bearing N-*MYC* amplification (Figure 1g). On the other hand, NLRR1 was undetectable in primary neuroblastomas carrying a single copy of *N-MYC* (data not shown). In addition, Spearman's rank correlation coefficient between *NLRR1* and *MYCN* mRNA expression in 136 primary neuroblastomas was 0.42 ($P<0.0001$) as shown in the scatter plot of Supplementary Figure S1, suggesting that *NLRR1* and *MYCN* expression in primary tumors is also positively correlated.

To address whether N-MYC could enhance the transcription of *NLRR1*, HeLa cells were transfected with or without the increasing amounts of the expression plasmid encoding N-MYC. As clearly shown in Supplementary Figure S2, N-MYC had an ability to transactivate the endogenous *NLRR1* in a dose-dependent manner. In contrast, N-MYC had undetectable effects on expression levels of the endogenous *NLRR2* (data not shown). Intriguingly, c-myc was also capable to transactivate the endogenous *NLRR1* (Supplementary Figure S2). Expression levels of *cyclin* E were examined as a positive control. As it has been well established that N-MYC recognizes and binds to so-called E-box (5′-CACGTG-3′), we sought to find out the putative E-box sequence(s) within 5′-upstream region as well as intron 1 of *NLRR1* gene. Finally, we found out three (E-1, E-2 and E-3) and two candidate E-boxes (E-4 and E-5) within 5′-upstream region and intron 1 of *NLRR1* gene, respectively (Figure 2a). To investigate whether these canonical E-boxes could respond to N-MYC, we subcloned genomic fragments containing each of these putative E-boxes into luciferase reporter plasmid to give pluc-E1, pluc-E2, pluc-E3, pluc-E4 and pluc-E5. SK-N-AS cells carrying a single copy of N-*MYC* were co-transfected with the constant amount of the expression plasmid for N-MYC and *Renilla* luciferase reporter plasmid together with the indicated luciferase reporter plasmids. At 48 h after transfection, cells were lysed and their luciferase activities were measured. As shown in Figure 2b, E-1 and E-4 boxes showed the relatively higher luciferase activities than those of the remaining putative E-box-containing fragments. Similar results were also obtained in mouse neuroblastoma Neuro2a cells (data not shown). Thus, we focused our attention on E-1 and E-4 boxes. To verify the functional significance of E-1 and/or E4 box, we have disrupted E-1 or E-4 box to give pluc-E1Δ or pluc-E4Δ luciferase reporter construct. Luciferase reporter assays demonstrated that pluc-E1Δ and pluc-E4Δ do not respond to exogenously expressed N-MYC (Figure 2c). These results indicate that E-1 and E-4 boxes are the functional elements involved in N-MYC-dependent transcriptional activation of *NLRR1*.

To ask whether N-MYC could be recruited onto E-1 and/or E-4 box in cells, we performed chromatin immunoprecipitation (ChIP) assays. Cross-linked chromatin prepared from the indicated cells was immunoprecipitated with normal mouse serum or with monoclonal anti-N-MYC antibody. Under our experimental conditions, an average length of sonicated genomic DNA fragments was 200–800 nucleotides in length (data not shown). The genomic DNA was purified from immunoprecipitates and amplified by PCR. As shown in Figure 2d, the estimated sizes of PCR products containing E-1 or E-4 box were detectable in IMR-32, SAN and CHP134 cells with N-*MYC* amplification, whereas our ChIP assays did not detect the estimated PCR products in SK-N-AS and SH-SY5Y cells bearing a single copy of N-*MYC*. In addition, we could not detect the efficient recruitment of N-MYC onto E-3 box that did not respond to exogenously expressed N-MYC. Consistent with these results, the anti-N-MYC immunoprecipitates prepared from Tet21N cells maintained in the absence of Tc contained the genomic fragments encompassing E-1 and E-4 boxes. In a sharp contrast, genomic fragment including E-3 box was not detectable in the anti-N-MYC immunoprecipitates prepared from Tet21N cells cultured in the absence of Tc. These observations suggest that N-MYC is recruited onto E-1 and E-4 boxes of *NLRR1* gene in cells.

We next examined a possible effect of NLRR1 on cell growth of neuroblastoma cells. SK-N-BE cells were transfected with the empty plasmid or with the expression plasmid for Myc-tagged NLRR1 (NLRR1-Myc). At 48 h after transfection, cells were transferred into fresh medium containing G418 for 2 weeks.

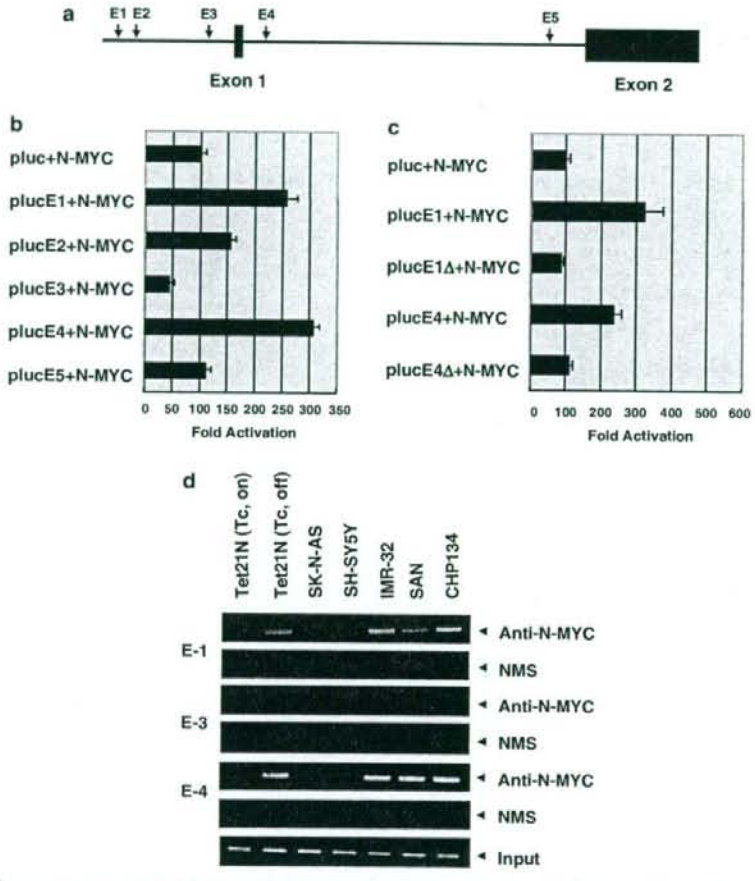

Figure 2 Luciferase reporter analysis. (**a**) Schematic drawing of the 5′-upstream region and intron 1 of human Neuronal leucine-rich repeat protein-1 (*NLRR1*) gene. Exons 1 and 2 were indicated by solid boxes. The positions of putative E-boxes were indicated by arrows. (**b**) Luciferase reporter assays. SK-N-AS cells were co-transfected with the constant amount of N-MYC-expression plasmid (100 ng), *Renilla* luciferase reporter plasmid (pRL-TK, 10 ng) and luciferase reporter plasmid containing E-1, E-2, E-3, E-4 or E-5 box (100 ng). Total amount of plasmid DNA per transfection was kept constant (510 ng) with pcDNA3. At 48 h after transfection, cells were lysed and their luciferase activities were measured by Dual-Luciferase reporter system (Promega, Madison, WI, USA). The firefly luminescence signal was normalized based on the *Renilla* luminescence signal. The results were obtained at least three independent experiments. (**c**) E-1 and E-4 boxes are required for N-MYC-dependent transactivation of *NLRR1* promoter. SK-N-AS cells were co-transfected with the constant amount of the expression plasmid for N-MYC (100 ng), pRL-TK (10 ng) and luciferase reporter plasmid lacking E-1 (pluc-E1Δ) or E-4 box (pluc-E4Δ). At 48 h after transfection, cells were lysed and their luciferase activities were measured as in (**b**). (**d**) N-MYC is efficiently recruited onto E-1 and E-4 boxes. Chromatin immunoprecipitation (ChIP) assays were carried out using chromatin immunoprecipitation assay kit provided from Upstate (Charlottesville, VA, USA). In brief, the indicated cells were cross-linked with formaldehyde and cross-linked chromatin was sonicated followed by immunoprecipitation with normal mouse serum (NMS) or with monoclonal anti-N-MYC antibody. Genomic DNAs were purified from the immunoprecipitates and subjected to PCR to amplify the genomic region containing E-1, E-3 and E-4 boxes. The oligonucleotide primer sequences used in this study are as follows: E-1, 5′-AAGTTGGATTTGATGACTGATACG-3′ (sense) and 5′-AGGCAAGAGACCATGTGCAGGAG-3′ (antisense); E-3, 5′-ATGAATCGAACAGTGGAGAGAC-3′ (sense) and 5′-AATGCTTAGGACAGTGCTTAG-3′ (antisense); E-4, 5′-TGTCTA ACATTAGCTGCGTGACC-3′ (sense) and 5′-AATGCTGTTCCGTGAATAGGTTC-3′ (antisense).

Drug-resistant cells were collected and their growth was examined. As shown in Figure 3a, exogenous NLRR1-Myc was expressed in drug-resistant cells transfected with NLRR1-Myc expression plasmid. Of note, NLRR1-Myc transfectants displayed an accelerated proliferation as compared with the control transfectants ($P<0.01$; Figure 3b). To investigate the possible role of the endogenous NLRR1, we have designed small-interfering RNA (siRNA) against NLRR1. As shown in Figure 3c, siRNA-targeting NLRR1 significantly downregulated the expression levels of the endogenous NLRR1 in SK-N-BE cells. As expected, siRNA-mediated knockdown of the endogenous NLRR1 significantly reduced the rate of cell growth as compared

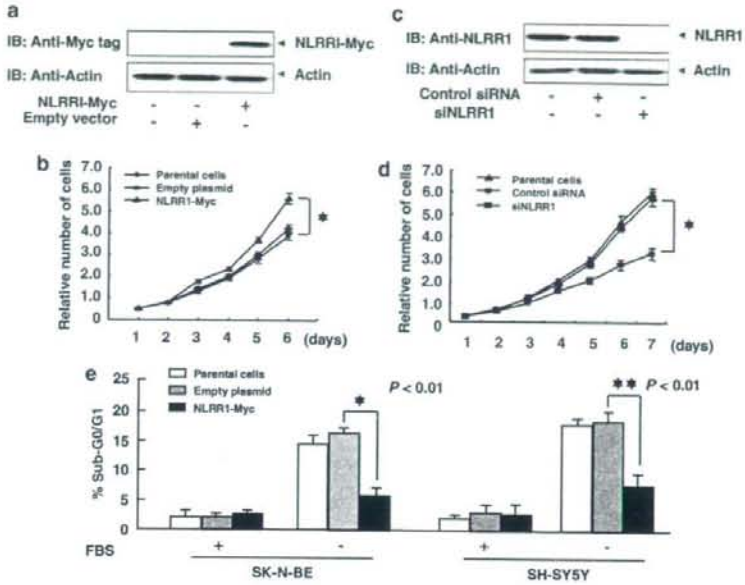

Figure 3 Neuronal leucine-rich repeat protein-1 (NLRR1) promotes cell proliferation. (**a**) Exogenous expression of NLRR1-Myc in SK-N-BE cells. SK-N-BE cells were transfected with the empty plasmid or with the expression plasmid for Myc-tagged NLRR1 (NLRR1-Myc) using Lipofectamine 2000 transfection reagent (Invitrogen, Carlsbad, CA, USA). At 48 h after transfection, cells were transferred into fresh medium containing G418 (600 μg/ml). After 2 weeks of selection, drug-resistant cells were harvested and analysed for the expression of exogenous NLRR1-Myc by immunoblotting with anti-Myc tag (PL14, Medical & Biological Laboratories, Nagoya, Japan) antibody. (**b**) Growth curves. Parental cells, control transfectants and NLRR1-Myc transfectants were seeded at a density of 1×10^5 cells per cell culture dish and allowed to attach overnight (day 1). At the indicated time points after seeding the cells, number of viable cells were measured and presented by graphs. Solid diamonds, squares and triangles indicate parental cells, control and NLRR1-Myc transfectants, respectively. $^*P<0.01$. (**c**) Small-interfering RNA (siRNA)-mediated knockdown of the endogenous NLRR1. SK-N-BE cells were transfected with control siRNA or with siRNA against NLRR1 (20 nM, Takara, Ohtsu, Japan) using Lipofectamine RNAiMAX (Invitrogen). At 48 h after transfection, cell lysates were prepared and subjected to immunoblotting with anti-NLRR1 antibody. (**d**) Growth curves. SK-N-BE cells were transfected as in (**c**). At 24 h after transfection, attached cells were collected and seeded at a density of 1×10^5 cells per cell culture plates. At the indicated time points after seeding the cells, number of viable cells were measured and presented by graphs. Solid triangles, circles and squares indicate parental cells, control transfectants and NLRR1-knocked down cells, respectively. $^*P<0.01$. (**e**) NLRR1 has an anti-apoptotic potential in response to fetal bovine serum (FBS) starvation. SK-N-BE and SH-SY5Y cells were transfected with the empty plasmid or with the expression plasmid encoding NLRR1-Myc. At 48 h after transfection, cells were transferred into fresh medium containing G418 (600 μg/ml). After 2 weeks of selection, drug-resistant cells were harvested and cultured in the presence or absence of FBS. At 24 h after treatment, floating and attached cells were collected, stained with propidium iodide (PI) and their cell-cycle distributions were analysed by fluorescence-activated cell sorting (FACS, Becton Dickinson, Mountain View, CA, USA). Results obtained by FACS analysis were presented by graphs. Open, gray and solid boxes indicate parental cells, control transfectants and NLRR1-Myc-expressing transfectants, respectively. $^*P<0.01$, $^{**}P<0.01$.

with the control cells ($P<0.01$; Figure 3d), indicating that NLRR1 has an ability to promote cell growth in neuroblastoma.

As described previously (Hamano *et al*., 2004), *NLRR1* was expressed at significantly higher levels in unfavorable neuroblastoma than favorable one, indicating that NLRR1 might have an anti-apoptotic activity. To address this issue, SK-N-BE and SH-SY5Y cells were transfected with the empty plasmid or with the expression plasmid for NLRR1-Myc. At 48 h after transfection, cells were exposed to G418 for 2 weeks. Drug-resistant cells were collected and cultured in the presence or absence of fetal bovine serum (FBS). At 24 h after FBS starvation, floating and attached cells were harvested, stained with propidium iodide and measured number of cells with sub-G_0/G_1 DNA content by fluorescence-activated cell sorting (FACS) analysis. As shown in Figure 3e, FBS deprivation increased number of parental and control SK-N-BE cells with sub-G_0/G_1 DNA content as compared with those cultured in the presence of FBS, whereas enforced expression of NLRR1-Myc significantly decreased number of cells with sub-G_0/G_1 DNA content relative to parental and control cells under FBS deprivation. Similar results were also obtained in SH-SY5Y cells (Figure 3e).

In support with these results, cleaved caspase-3 was detectable in control SK-N-AS transfectants maintained in the absence of FBS, whereas we did not detect cleaved caspase-3 in NLRR1-Myc transfectants under FBS deprivation (Figure 4a). Cleaved caspase-3 was also detected in parental cells in the absence of FBS (Figure 4b). In addition, cleaved poly-(ADP-ribose)

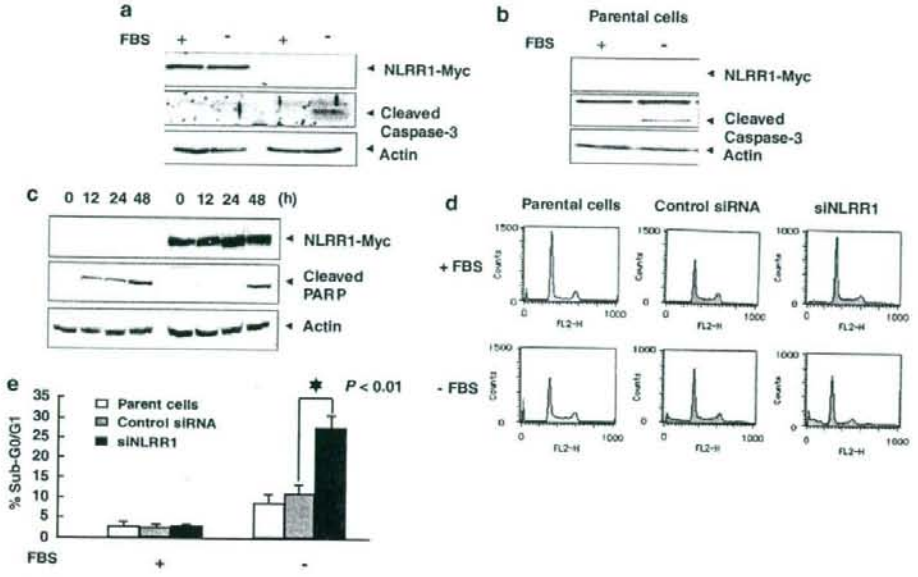

Figure 4 Neuronal leucine-rich repeat protein-1 (NLRR1) is involved in the regulation of serum starvation-induced apoptosis. (**a**) NLRR1 inhibits the activation of caspase-3. Control transfectants and NLRR1-Myc-expressing transfectants derived from SK-N-AS cells were cultured in the presence or absence of fetal bovine serum (FBS). At 24 h after the treatment, cell lysates were prepared and processed for immunoblotting with anti-Myc tag (top) or with anti-caspase-3 (Cell Signaling, Beverly, MA, USA) antibody (middle). Actin was used as a loading control (bottom). (**b**) Deprivation of FBS induces cleavage of caspase-3 in SK-N-AS cells. SK-N-AS cells were cultured in the presence or in the absence of FBS. At 24 h after the treatment, cell lysates were prepared and subjected to immunoblotting with the indicated antibodies. (**c**) Effect of NLRR1 on cleavage of poly-(ADP-ribose) polymerase (PARP) in response to FBS deprivation. Control transfectants (left) and NLRR1-Myc-expressing transfectants (right) were maintained in the absence of FBS. At the indicated time points after FBS withdrawal, cell lysates were prepared and analysed for the expression of NLRR1-Myc (top) as well as the proteolytic cleavage of PARP by immunoblotting with anti-PARP (Cell Signaling) antibody (middle). Actin was used as a loading control (bottom). (**d**, **e**) Small-interfering RNA (siRNA)-mediated knockdown of the endogenous NLRR1 enhances apoptosis in response to FBS starvation. Tet21N cells were grown in the fresh medium without tetracycline (Tc) and transfected with control siRNA or with siRNA against NLRR1. At 48 h after transfection, cells were transferred into fresh medium without Tc and FBS. At 24 h after FBS starvation, floating and attached cells were collected, stained with propidium iodide (PI) and their cell-cycle distributions were examined by fluorescence-activated cell sorting (FACS) (**d**). Results obtained by FACS analysis were presented by graphs. Open, gray and solid boxes indicate parental cells, control transfectants and NLRR1-knocked down transfectants, respectively (**e**). $^{*}P<0.01$.

polymerase (PARP) that is one of caspase-3 substrates (Truscott *et al.*, 2007), started to be observed in control transfectants 12 h after FBS starvation (Figure 4c). On the other hand, the kinetics for cleavage of PARP was delayed in NLRR1-Myc transfectants. Under our experimental conditions, control SK-N-AS transfectants underwent apoptosis in response to FBS deprivation, whereas enforced expression of NLRR1-Myc in SK-N-AS cells inhibited the FBS deprivation-induced apoptosis (data not shown). These findings suggest that NLRR1 confers resistance of neuroblastoma cells to FBS starvation-induced apoptosis.

To further confirm this notion, Tet21N cells were maintained in the absence of Tc and then transfected with control siRNA or with siRNA against NLRR1. At 48 h after transfection, cells were cultured in the absence of FBS for 24 h and then their cell-cycle distributions were analysed by FACS. As shown in Figures 4d and e, siRNA-mediated knockdown of the endogenous NLRR1 resulted in a significant increase in number of cells with sub-G_0/G_1 DNA content in response to FBS deprivation as compared with parental cells and control transfectants. Collectively, our present results strongly suggest that NLRR1 is a novel transcriptional target of N-MYC and has a growth-promoting as well as anti-apoptotic potential.

Small-interfering RNA-mediated knockdown of the endogenous NLRR1 in SK-N-BE cells bearing N-*MYC* amplification resulted in a significant decrease in the rate of cell growth. Furthermore, enforced expression of NLRR1-Myc conferred resistance of SK-N-BE and SH-SY5Y cells to FBS deprivation-mediated apoptosis. In contrast, siRNA-mediated knockdown of the endogenous NLRR1 led to an increase in number of cells with sub-G_0/G_1 DNA content in response to FBS deprivation. In addition, NLRR1-Myc blocked the activation of caspase-3 in SK-N-AS cells exposed to FBS depletion and thereby inhibiting the proteolytic cleavage of PARP. Thus, it is conceivable that NLRR1 inhibits the mitochondria-dependent intrinsic apoptotic pathway of caspase activation (Degterev *et al.*, 2003). As

reported previously (Hamano *et al*., 2004), expression levels of *NLRR1* in unfavorable neuroblastoma were significantly higher than those of favorable one and closely correlated with poor clinical outcome. As aggressive neuroblastoma displays unfavorable clinical outcome despite intensive chemotherapy (Brodeur and Nakagawara, 1992), it is likely that N-MYC-mediated induction of NLRR1 is involved in the regulation of chemoresistant phenotypes of certain neuroblastomas. However, precise molecular mechanisms behind NLRR1-mediated growth promotion and anti-apoptotic effect in response to FBS starvation remain unclear. Further studies should be necessary to address this issue.

According to our present results, N-MYC-dependent transcriptional induction of *NLRR1* was observed in neuroblastoma cell lines. Furthermore, expression levels of *NLRR1* significantly correlated with those of N-*MYC* in primary neuroblastomas. Intriguingly, the enforced expression of N-MYC in HeLa cells also induced the expression of NLRR1, indicating that N-MYC-mediated transcriptional activation of *NLRR1* is not restricted to neuroblastoma cells. As described previously (Blackwood and Eisenman, 1991; Torres *et al*., 1992), c-myc/Max heterodimeric complex also recognizes and binds to E-box. Like N-MYC, c-myc had an ability to induce the expression of NLRR1. Of note, our luciferase reporter assays indicated that E-1 and E-4 boxes are required for N-MYC-dependent activation of *NLRR1* promoter, whereas E-3 box does not respond to N-MYC. Similar results were also obtained in cells transfected with the expression plasmid for c-myc (data not shown). As described previously (Hamano *et al*., 2004), *NLRR1* was expressed ubiquitously in human tissues. Among them, higher levels of *NLRR1* expression were observed in nerve tissues. Considering that N-*MYC* expression is largely restricted to embryonic tissues as well as neuroendocrine tumors, whereas c-*myc* is expressed in a wide variety of tissues as well as tumors (Boon *et al*., 2001), N-MYC and c-myc might act as transcription factors for *NLRR1* in a cell-type-dependent manner under physiological conditions.

In the present study, we have found that *NLRR1* is one of direct transcriptional targets of oncogenic N-MYC and is important in the regulation of cell proliferation and the protection of cells from FBS deprivation-induced apoptosis in neuroblastoma cells. In support with this notion, there exists a positive correlation between expression levels of N-*MYC* and *NLRR1* in primary neuroblastomas. To our knowledge, NLRR1 is a first membrane protein whose expression levels are directly regulated by N-MYC. Thus, our present findings might provide a novel insight into understanding molecular mechanisms behind genesis and development of aggressive neuroblastoma with N-*MYC* amplification.

Acknowledgements

We are grateful to Dr M Schwab for providing the expression plasmid for N-MYC. We thank Ms Y Nakamura for technical assistance. This work was supported in part by a Grant-in-Aid from the Ministry of Health, Labour and Welfare for Third Term Comprehensive Control Research for Cancer, a Grant-in-Aid for Scientific Research on Priority Areas from the Ministry of Education, Culture, Sports, Science and Technology, Japan, a Grant-in-Aid for Scientific Research from Japan Society for the Promotion of Science, Uehara Memorial Foundation and Hisamitsu Pharmaceutical Co.

References

Alex R, Sozeri O, Meyer S, Dildrop R. (1992). Determination of the DNA sequence recognized by the bHLH-zip domain of the N-Myc protein. *Nucleic Acids Res* **20**: 2257 2263.

Bando T, Sekine K, Kobayashi S, Watabe AM, Rump A, Tanaka M *et al*. (2005). Neuronal leucine-rich repeat protein 4 functions in hippocampus-dependent long-lasting memory. *Mol Cell Biol* **25**: 4166 4175.

Bernards R, Dessain SK, Weinberg RA. (1986). N-myc amplification causes down-modulation of MHC class I antigen expression in neuroblastoma. *Cell* **47**: 667 674.

Blackwood EM, Eisenman RN. (1991). Max: a helix-loop-helix zipper protein that forms a sequence-specific DNA binding complex with Myc. *Science* **251**: 1211 1217.

Blackwood EM, Kretzner I, Eisenman RN. (1992). Myc and Max function as a nucleoprotein complex. *Curr Opin Genet Dev* **2**: 227 235.

Boon K, Caron HN, van Asperen R, Valentijn L, Hermus MC, van Sluis P *et al*. (2001). N-myc enhances the expression of a large set of genes functioning ribosome biogenesis and protein synthesis. *EMBO J* **20**: 1383 1393.

Brodeur GM, Nakagawara A. (1992). Molecular basis of clinical heterogeneity in neuroblastoma. *Am J Pediatr Hematol Oncol* **14**: 111 116.

Degterev A, Boyce M, Yuan J. (2003). A decade of caspases. *Oncogene* **22**: 8543 8567.

Fukamachi K, Matsuoka Y, Ohno H, Hamaguchi T, Tsuda H. (2002). Neuronal leucine-rich repeat protein-3 amplifies MAPK activation by epidermal growth factor through a carboxyl-terminal region containing endocytosis motifs. *J Biol Chem* **277**: 43549 43552.

Hamano S, Ohira M, Isogai E, Nakada K, Nakagawara A. (2004). Identification of novel human neuronal leucine-rich repeat (h*NLRR*) family, genes and inverse association of expression of *Nbla10449/hNLRR-1* and *Nbla10677/hNLRR-3* with the prognosis of primary neuroblastomas. *Int J Oncol* **24**: 1457 1466.

Kohl NE, Kanda N, Schreck RR, Bruns G, Latt SA, Gilbert F *et al*. (1983). Transposition and amplification of oncogene-related sequences in human neuroblastomas. *Cell* **35**: 359 367.

Kouzarides T, Ziff E. (1988). The role of the leucine zipper in the fos-jun interaction. *Nature* **336**: 646 651.

Landschulz WH, Johnson PF, McKnight S. (1988). The leucine zipper: a hypothetical structure common to a new class of DNA binding proteins. *Science* **240**: 1759 1764.

Lasorella A, Noseda M, Beyna M, Iavarone A. (2000). Id2 is a retinoblastoma protein target and mediates signaling by Myc oncoproteins. *Nature* **407**: 592 598.

Lutz W, Stohr M, Schurmann J, Wenzel A, Lohr A, Schwab M. (1996). Conditional expression of N-myc in human neuroblastoma cells increases expression of a-prothymosin and ornithine decarboxylase and accelerates progression into S-phase early after mitogenic stimulation of quiescent cells. *Oncogene* **13**: 803 812.

Murre C, Schonleber McCaw P, Baltimore D. (1989). A new DNA binding and dimerization motif in immunoglobulin enhancer binding, daughterless, MyoD, and myc proteins. *Cell* **56**: 777 783.

Negroni A, Scarpa S, Romeo A, Ferrari S, Modesti A, Raschella G. (1991). Decrease of proliferation rate and induction of differentiation by a MYCN antisense DNA oligomer in a human neuroblastoma cell line. *Cell Growth Differ* **2**: 511 518.

Schwab M, Alitalo K, Klempnauer KH, Varmus HE, Bishop JM, Gilbert F *et al.* (1983). Amplified DNA with limited homology to *myc* cellular oncogene is shared by human neuroblastoma cell lines and a neuroblastoma tumour. *Nature* **305**: 245 248.

Seeger RC, Brodeur GM, Sather H, Dalton A, Siegel SE, Wong KY *et al.* (1985). Association of multiple copies of the N-myc oncogene with rapid progression of neuroblastomas. *N Engl J Med* **313**: 1111 1116.

Slack A, Chen Z, Tonelli R, Pule M, Hunt L, Pession A *et al.* (2005). The p53 regulatory gene MDM2 is a direct transcriptional target of MYCN in neuroblastoma. *Proc Natl Acad Sci USA* **102**: 731 736.

Taguchi A, Wanaka A, Mori T, Matsumoto K, Imai Y, Takagi T *et al.* (1996). Molecular cloning of novel leucine-rich repeat proteins and their expression in the developing mouse nervous system. *Brain Res Mol Brain Res* **35**: 31 40.

Taniguchi H, Tohyama A, Takagi T. (1996). Cloning and expression of a novel gene for a protein with leucine-rich repeats in the developing mouse nervous system. *Brain Res Mol Brain Res* **36**: 45 52.

Torres R, Schreiber-Agus N, Morgenbesser SD, DePinho RA. (1992). Myc and Max: a putative transcriptional complex in search of a cellular target. *Curr Opin Cell Biol* **4**: 468 474.

Truscott M, Denault JB, Goulet B, Leduy L, Salvesen GS, Nepveu A. (2007). Carboxy-terminal proteolytic processing of CUX1 by a caspase enables transcriptional activation in proliferating cells. *J Biol Chem* **282**: 30216 30226.

Wang J, Xie I, Allan S, Beach D, Hannon G. (1998). Myc activates telomerase. *Genes Dev* **12**: 1769 1774.

Weiss WA, Aldape K, Mohapatra G, Feuerstein BG, Bishop JM. (1997). Targeted expression of MYCN causes neuroblastoma in transgenic mice. *EMBO J* **16**: 2985 2995.

Supplementary Information accompanies the paper on the Oncogene website (http://www.nature.com/onc)

Int. J. Cancer: **123**, 2087–2094 (2008)

Expression of *TSLC1*, a candidate tumor suppressor gene mapped to chromosome 11q23, is downregulated in unfavorable neuroblastoma without promoter hypermethylation

Kiyohiro Ando[1], Miki Ohira[1], Toshinori Ozaki[1], Atsuko Nakagawa[2], Kohei Akazawa[3], Yusuke Suenaga[1], Yohko Nakamura[1], Tadayuki Koda[4], Takehiko Kamijo[1], Yoshinori Murakami[5] and Akira Nakagawara[1]*

[1]*Division of Biochemistry, Chiba Cancer Center Research Institute, Chiba, Japan*
[2]*Division of Clinical Laboratory, National Center for Child Health and Development, Tokyo, Japan*
[3]*Division of Medical Information, Niigata University Medical and Dental Hospital, Niigata, Japan*
[4]*Center for Functional Genomics, Hisamitsu Pharmaceutical Co. Inc., Chiba, Japan*
[5]*Division of Molecular Pathology, Department of Cancer Biology, Institute of Medical Science, The University of Tokyo, Tokyo, Japan*

Although it has been well documented that loss of human chromosome 11q is frequently observed in primary neuroblastomas, the smallest region of overlap (SRO) has not yet been precisely identified. Previously, we performed array-comparative genomic hybridization (array-CGH) analysis for 236 primary neuroblastomas to search for genomic aberrations with high-resolution. In our study, we have identified the SRO of deletion (10-Mb or less) at 11q23. Within this region, there exists a *TSLC1/IGSF4/CADM1* gene (*Tumor suppressor in lung cancer 1/Immunoglobulin superfamily 4/Cell adhesion molecule 1*), which has been identified as a putative tumor suppressor gene for lung and some other cancers. Consistent with previous observations, we have found that 35% of primary neuroblastomas harbor loss of heterozygosity (LOH) on *TSLC1* locus. In contrast to other cancers, we could not detect the hypermethylation in its promoter region in primary neuroblastomas as well as neuroblastoma-derived cell lines. The clinicopathological analysis demonstrated that *TSLC1* expression levels significantly correlate with stage, Shimada's pathological classification, *MYCN* amplification status, *TrkA* expression levels and DNA index in primary neuroblastomas. The immunohistochemical analysis showed that TSLC1 is remarkably reduced in unfavorable neuroblastomas. Furthermore, decreased expression levels of *TSLC1* were significantly associated with a poor prognosis in 108 patients with neuroblastoma. Additionally, TSLC1 reduced cell proliferation in human neuroblastoma SH-SY5Y cells. Collectively, our present findings suggest that *TSLC1* acts as a candidate tumor suppressor gene for neuroblastoma.

Key words: *TSLC1/IGSF4/CADM1*; neuroblastoma; 11q23; tumor suppressor

Neuroblastoma is one of the most common solid tumors in childhood and originates from the sympathoadrenal lineage of neural crest. Its biological as well as clinical behavior is highly heterogeneous in different prognostic subsets. Tumors found in patients under 1 year of age often regress spontaneously or differentiate and result in a favorable prognosis.[1] In a sharp contrast to these favorable neuroblastomas, tumors found in patients over 1 year of age are often aggressive with an unfavorable prognosis despite an intensive therapy. A large number of multiple genomic aberrations including DNA index, *MYCN* amplification status, allelic loss of the distal part of chromosome 1p and the gain of chromosome 17q have been identified in neuroblastoma.[2,3]

Alternatively, allelic loss of 11q has been frequently observed in advanced stage of neuroblastoma with single copy of *MYCN*. Indeed, 30% of tumors harbor allelic loss of 11q, and it might be an independent prognostic indicator for clinically high-risk patients without *MYCN* amplification.[4,5] Aberrant deletions of 11q often occur in a distal part of its long arm. Although several lines of evidence delineated the smallest region of overlaps (SRO) of deletions at 11q, it remains unclear whether there could exist a candidate tumor suppressor gene(s) implicated in biological and clinical behaviors of neuroblastoma.[6,7] Recently, we have performed an array-comparative genomic hybridization (array-CGH) analysis using 236 primary neuroblastomas and finally defined the SRO (10-Mb or less) at 11q23.[3,8] During our extensive search for the already identified candidate tumor suppressor gene(s) within this region, we have found that *TSLC1/IGSF4/CADM1* gene is localized within this region.

TSLC1 gene has been originally identified as a putative tumor suppressor for non-small-cell lung cancer (NSCLC) located at chromosome 11q23 by functional complementation strategy of a human lung cancer cell line. The downregulation of *TSLC1* gene was frequently detected in various human cancers including NSCLC, prostate cancers, hepatocellular carcinomas and pancreatic cancers through its allelic loss as well as hypermethylation of its promoter region. In spite of an extensive mutation search, only 2 inactivating *TSLC1* gene mutations were detected in 161 primary tumors and tumor-derived cell lines, suggesting that *TSLC1* is rarely mutated in human cancers.[9] *TSLC1* encodes a single membrane-spanning glycoprotein involved in cell–cell adhesion through homophilic trans interaction.[10] Accumulating evidence indicates that TSLC1 is significantly associated with biological aggressiveness and metastasis of certain types of cancer,[11–16] whereas the functional significance of TSLC1 in neuroblastoma remains elusive.

In the present study, we have further delineated the SRO of 11q deletion in primary neuroblastoma by array-CGH analysis and finally identified *TSLC1* gene within this region. In contrast to the other cancers, hypermethylation of *TSLC1* promoter region was undetectable in neuroblastoma. Intriguingly, the expression levels of *TSLC1* gene were highly associated with clinical stage, Shimada's pathological classification, *MYCN* amplification status, *TrkA* expression levels and DNA index in primary neuroblastoma.

Additional Supporting Information may be found in the online version of this article.

Abbreviations: array-CGH, array-comparative genomic hybridization; BAC, bacterial artificial chromosome; LOH, loss of heterozygosity; PARP, poly(ADP-ribose) polymerase; SRO, smallest region of overlap; STS, sequence-tagged-site; TSA, trichostatin A; TSLC1, tumor suppressor in lung cancer 1.

Grant sponsors: Ministry of Health, Labour and Welfare for Third Term Comprehensive Control Research for Cancer; Ministry of Education, Culture, Sports, Science and Technology, Japan; Scientific Research from Japan Society for the Promotion of Science.

***Correspondence to:** Chiba Cancer Center Research Institute, 666-2 Nitona, Chuo-ku, Chiba 260-8717, Fax: +81-43-265-4459.
E-mail: akiranak@chiba-cc.jp

Received 21 February 2008; Accepted after revision 19 May 2008
DOI 10.1002/ijc.23776
Published online 22 August 2008 in Wiley InterScience (www.interscience.wiley.com).